A TECHNICAL REPORT
ENTITLED

STRUCTURAL SIMILITUDE AND SCALING LAWS FOR LAMINATED BEAM-PLATES

SUBMITTED TO

THE NASA–LANGLEY RESEARCH CENTER
HAMPTON, VIRGINIA

BY

GEORGE J. SIMITSES* AND JALIL REZAEEPAZHAND†

AEROSPACE ENGINEERING AND ENGINEERING MECHANICS
UNIVERSITY OF CINCINNATI
CINCINNATI, OHIO 45221

(NASA Grant NAG–1–1280)

* Professor and Head.
† Graduate Research Assistant.

Abstract

This study describes the establishment of similarity conditions between two structural systems. Similarity conditions provide the relationship between a scale model and its prototype, and can be used to predict the behavior of the prototype by extrapolating the experimental data of the corresponding small scale model. Since satisfying all the similarity conditions simultaneously is difficult or even impossible, distorted models with partial similarity (with at least one similarity condition relaxed) are more practical. Establishing similarity conditions, based on both dimensional analysis and direct use of governing equations, is discussed and the possibility of designing distorted models is investigated. The method is demonstrated through analysis of the cylindrical bending of orthotropic laminated beam–plates subjected to transverse line loads.

Contents

List of Figures

List of Tables

NOMENCLATURE

a	*plate length*
A_{ij}	*laminate extensional stiffnesses*
b	*plate width*
B_{ij}	*laminate coupling stiffnesses*
D	*beam flexural stiffness*
D_{ij}	*laminate flexural stiffnesses*
E, E_{ij}	*Young's moduli of elasticity*
h	*total laminate thickness*
I	*second moment of area*
k	*elastic spring stiffness*
k_{xx}, k_{yy}	*bending curvatures in the laminate*
k_{xy}	*twisting curvature in the laminate*
L	*column length*
M_{xx}	*moment resultant*
N_{xx}	*stress resultant*
$\bar{N}_{xx}$	*uniform compressive load*
P	*axial force*
q_0	*transverse load intensity*
$Q_{ij}, \bar{Q}_{ij}$	*lamina stiffness elements*
t	*ply thickness*
u, v, w	*reference surface displacements*
x, y, z	*reference axes*
z	*distance from the midplane in the thickness direction*
δ	*deflection at middle of beam*
$\gamma^0{}_{xy}$	*midplane shear strain in the laminate*
$\epsilon^0{}_{xx}, \epsilon^0{}_{yy}$	*midplane extensional strains in the laminate*

θ	*fiber orintation angle*
Λ	*transformation matrix*
λ_i	*scale factor*
ν, ν_{ij}	*Poission's ratios*
π_i	*π-terms or π-products*
$\sigma_{xx}^{(k)}, \sigma_{yy}^{(k)}$	*normal stresses in the k^{th} lamina*
$\tau_{xy}^{(k)}$	*shear stress in the k^{th} lamina*

SUBSCRIPTS

exp.	:	*experimental*
m	:	*model*
p	:	*prototype*
pr.	:	*predicted*
th.	:	*theoretical*

Chapter 1

INTRODUCTION

1.1 Introduction

Before production, any new design is subjected to many investigations through theoretical analyses and experimental verification. As a system becomes more complex, assumptions are usually made in order to formulate a mathematical model for the system . In the absence of a complete design base, a new system requires extensive experimental evaluation until it gains the necessary reliability and desired performance. Since most of these tests are destructive, many test specimens are needed (Morton,1988).

For large and "oversize" systems, such as tall buildings , dams, bridges, spacecraft, airplanes, and space stations, creating the actual working conditions for testing the prototype most of the time is impossible, as in providing a "zero gravitional accelaration condition " on the ground for testing large space stations or antennas (Letchworth et al., 1988 and McGowan et al,1990). Even when a prototype test is possible, it is expensive, time consuming , and difficult to control. Thus, it is extremely useful if a prototype can be replaced by a similar scale model which is much easier to work with. The only possible way to obtain experimental data of overall performance of such a system and the interaction of its elements is to design a small similar system (*scale model*) which replicates the behavior of the actual system (*prototype*). The accuracy of the behavior of the prototype , which is predicted from interpreting the test results of the model, is dependent on the relationship between the corresponding

variables and parameters of model and its prototype.

Similarity of systems requires that the relevant system parameters are identical and these systems are governed by unique set of characteristic equations. Thus, if a relation or equation of variables is written for a system, it is valid for all systems which are similar to it (Kline,1965). Each variable in a model is proportional to the corresponding variable of the prototype. This ratio, which has essential roles in predicting the relationship between model and its prototype, is called *scale factor* .

Since making a precise and adequate experiment is difficult and expensive, it is more convenient to run a series of experiments in nondimensional form of variables, the results of which can then be used for a similar system. Models, as a design aid, have been used for several years, but the use of scientific models which are based on dimensional analysis was first discussed in a paper by Rayleigh. Similarity conditions based on dimensional analysis have been used since Rayleigh's time (Macagno,1971), but the applicability of the theory of similitude to structural systems was first discussed by Goodier and Thomson (1944). They presented a systematic procedure for establishing similarity conditions based on dimensional analysis.

In establishing similarity conditions between the model and prototype two procedures can be used. The similarity conditions can be established either directly from the field equations of the system or, if it is a new phenomenon and the mathematical model of the system is not available, through dimensional analysis. In the second case, all of the variables and parameters which affect the behavior of the system must be known. By using dimensional analysis, an incomplete form of the characteristic equation of the system can be formulated. This equation is in terms of nondimensional products of variables and parameters of the system. Then, similarity conditions can be established on the basis of this equation.

The objective of this study is to discuss and demonstrate the establishment of the similarity relations between two structural systems. Similarity conditions provide the relationship between model and its prototype, and can be used to extrapolate the experimental data of a small and less expensive model in order to predict the behavior of the prototype. In all of our work in this area we will restict ourselves to

linearly elastic material behavior.

1.2 Literature Review

The scientific small scale model based on dimensional analysis, was first discused by Rayleigh(1915). He established the fundamentals of dimensional analysis based on Fourier's work. This principle has been reviewed and completed by Riabouchinsky, Buckingham, Bridgman, Bickhoff, and Langhaar. (for more detail see Macango, 1971).

The applicability of the theory of similitude to structural systems was first discused by Goodier and Thomson(1944) and later by Goodier in 1955. In the 50's and 60's many interesting books have been published in this area, Murphy(1950), Langhaar(1951), Sedov(1959), Kline(1965), Skoglund(1967). Most of these authors discussed similitude theory based on dimensional analysis. Kline(1965) gives a perspective of the method based on both, dimensional analysis and the direct use of the governing equations. Szucs (1980) is particularly thorough on the topic of the similitude theory. He explains the method with emphasis on the direct use of the governing equations of the system.

Many research activities have been conducted on modeling of dynamic and static behavior of structural systems, especially on modeling the reinforced concrete structures, (see Sabines and White (1966,1977), Harris et.al.(1966,1970)). Krawinkler et.al.(1978) described detailed model studies on earthquake resistance of structures and presented a comprehensive reference on the dynamic behavior of structures for seismic engineering analysis.

Since reinforced composite components require extensive experimental evaluation, there is a growing interest in small scale model testing. Morton (1988) discusses the application of scaling laws for impact-loaded Carbon-Fiber composite beams. His work is based on dimensional analysis. Qian et.al.(1990) conducted experimental studies of impact loaded composite plates, where the similarity conditions were obtained by considering the governing equations of the system.

In recent years, due to large dimensions and unique structural design of the proposed space station, small scale model testing and similitude analysis have been considered as the only option in order to gain experimental data. Letchworth et.al.(1988), Shih et.al.(1987), Hsu et.al.(1989), and McGowan et.al.(1990) discussed the possibility of scale model testing of space station geometries especially for vibration analysis.

Most of these studies have used complete similarity between model and prototype. The objectives of the investigation described herein are:

- explore two fundamental methods of similitude analysis
- create necessary similarity conditions in order to design an accurate distorted model
- evaluate the derived similarity conditions analytically and correlate the actual experimental data of the prototype with the small scale model predictions.

The experimental data of cylindrical bending of several beam-plates are used to support the applicability of the derived similarity conditions.

Chapter 2

THEORY OF SIMILITUDE

This chapter is devoted to consideration of foundations of the similitude theory. The meaning of similitude is explained, and two major methods of obtaining similarity conditions are discussed.

Similitude theory is concerned with establishing necessary and sufficient conditions of similarity between two phenomena. Establishing similarity between systems helps to predict the behavior of a system from the results of investigating other systems which have already been investigated or can be investigated more easily than the original system. Similitude among systems means similarity in behavior in some specific aspects. In other words, knowing how a given system responds to a specific input, the response of all similar systems to similar input can be predicted.

Euclid established the fundamental theory of similitude by defining geometric similarity for plane geometric figures. According to this theory, enlarging or contracting all dimensions of a figure by a constant ratio, which is called scale or similarity factor, forms figures which are similar to the original figure.

The behavior of a physical system depends on many parameters, i.e. geometry , material behavior, dynamic response, and energy characteristic of the system. The nature of any system can be modeled mathematically in term of its variables and parameters. A prototype and its scale model are two different systems with different parameters. The necessary and sufficient conditions of similitude between prototype and its scale model require that the mathematical model of the scale model can be transformed to that of the prototype by a bi-unique mapping or vice versa (Szucs,

1980). It means, if vectors X_p and X_m are the characteristic vectors of the prototype and model , then we can find a transformation matrix Λ such that

$$X_p = \Lambda X_m \quad or \quad X_m = \Lambda^{-1} X_p \tag{2.1}$$

The elements of vector X are all the parameters and variables of the system. A diagonal form of the transformation matrix Λ is the simplest form of transformation. The diagonal elements of the matrix are the scale factors of the pertinent element of the characteristic vector X.

$$\Lambda = \begin{bmatrix} \lambda_{x1} & 0 & \dots & 0 \\ 0 & \lambda_{x2} & \dots & 0 \\ \vdots & \vdots & \ddots & \vdots \\ 0 & 0 & \dots & \lambda_{xn} \end{bmatrix} \tag{2.2}$$

where $\lambda_{x_i} = \dfrac{x_{ip}}{x_{im}}$ denotes the scale factor of x_i. In general the transformation matrix is not diagonal.

Since similitude theory gives many alternative ways for investigating a system, it has been used in areas which primarily involved many experimental investigations. Two methods, dimensional analysis and direct use of governing equations are used to establish similitude between systems.

2.1 Dimensional Analysis

The principal purpose of dimensional analysis is to reduce the number of parameters by establishing product groups of variables (π-*terms*) such that all terms are mutually independent and dimensionless.

Rayleigh established the fundamentals of dimensional analysis based on Fourier's work. Riabouchinsky proved the fundamental theorems of dimensional analysis , and Buckingham reformulated Riabouchinsky's theorems. Buckingham's theorem was discussed and revised by Bridgman, Brickhoff, Langhaar, Van Driest, and Brand, and was named Buckingham's π-Theorem, or simply the π-Theorem (Macagno,1971). This theorem states that a given relation among n variables can be reduced to an equivalent relationship in terms of a complete set of $n - r$ dimensionless π-terms,

where r is the rank of the dimensional matrix.

$$\phi(x_1, x_2, x_3, \cdots, x_n) = 0 \quad or \quad \Phi(\pi_1, \pi_2, \cdots, \pi_{n-r}) = 0 \tag{2.3}$$

The function Φ is called *functional relation.* The functional relation need not be a known function of the system variables. Function Φ only shows the reduced form of relevant variables and does not give any information about the nature of the solution. Any physical system can be described in term of various combinations of fundamental quantities such as M(mass) , L(lenght) , F(force) , T (time), and secondary quantities such as v (velocity) ,σ (stress), A(area) etc. The first step is to choose an adequate set of fundamental quantities (dimensions). Then all variables can be described in this system, which is unique for that set of fundamental dimensions, and can change by choosing another set of dimensions. It is necessary that all pertinent parameters, even constants like the gravitational acceleration g, be included, otherwise the analysis leads to incorrect and incomplete results.

Barr(1983) has presented five methods for dimensional analysis. These are the Rayleigh method and various modifications such as the Buckingham method, the Echlon Matrix method, the Basic Stepwise method, and the Proportionalities method.

As an example consider the procedure for finding the buckling load of a simply supported elastic column with an elastic support at the middle (Figure 2.1). The relevant variables are:

variable	*dimensions*
w=deflection	L
L=span	L
E=modulus of elasticity	FL^{-2}
I=moment of inertia	L^4
k=spring stiffness	FL^{-1}
P=axial load	F

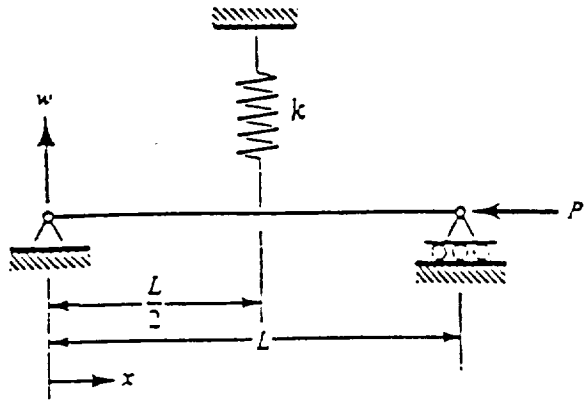

Figure 2.1: Simply Supported Column

$$\phi(w, L, E, I, k, P) = 0$$

The dimensional matrix and the resulting π-terms are [see Barr (1979) for details on the procedure]:

$$\begin{array}{c} \\ L \\ F \end{array} \begin{array}{c} \begin{array}{cccccc} L & E & w & I & k & P \end{array} \\ \begin{pmatrix} 1 & -2 & 1 & 4 & -1 & 0 \\ 0 & 1 & 0 & 0 & 1 & 1 \end{pmatrix} \end{array} \Rightarrow \begin{array}{c} \\ L \\ E \end{array} \begin{array}{c} \begin{array}{cccccc} L & E & w & I & k & P \end{array} \\ \begin{pmatrix} 1 & 0 & 1 & 4 & 1 & 2 \\ 0 & 1 & 0 & 0 & 1 & 1 \end{pmatrix} \end{array}$$

$$\pi_1 = \frac{w}{L} \quad , \pi_2 = \frac{I}{L^4} \quad , \pi_3 = \frac{k}{LE} \quad , \pi_4 = \frac{P}{EL^2}$$

By applying one of the dimensional analysis methods, a set of π-terms is calculated which is not unique and many other combinations of parameters can yield several sets of π-terms.

Since experimental control of some variables is easier than others, it is more convenient to have these variables only in one of the π-terms. Power products of π-terms are also nondimensional which can be used in place of the inadequate π-terms. The resulting π-terms can be written as

$$\phi(\pi_1, \pi_2, \pi_3, \pi_4) = 0$$

If π_1 involves the dependent variable, it can be written as a function of the other π-terms (independent variables).

$$\pi_1 = \Phi(\pi_2, \pi_3, \pi_4)$$

Similarity conditions require that the equations of two similar systems be the same. If the π-terms of the functional equation for two systems are the same, then $\Phi_1 = \Phi_2$ even if we don't know the functional equation completely. These equalities of π-terms which determine the conditions for which the two systems are similar, are called the similarity conditions or scaling laws for these systems and for specific phenomena.

$$\pi_{1p} = \Phi_p(\pi_{2p}, \pi_{3p}, \pi_{4p}) \quad , \quad \pi_{1m} = \Phi_m(\pi_{2m}, \pi_{3m}, \pi_{4m})$$

if $\pi_{im} = \pi_{ip} \quad for \quad i = 2, 3, 4$, then

$$\Phi_p(\pi_{2p}, \pi_{3p}, \pi_{4p}) = \Phi_m(\pi_{2m}, \pi_{3m}, \pi_{4m})$$

hence

$$\pi_{1m} = \pi_{1p}$$

Since these π-terms are combinations of geometric , dynamic, material, and kinematic parameters of the systems, the above equalities define different similarities, such as geometric , material, kinematic, and dynamic similarity (Schuring,1977).

2.2 Direct Use of Governing Equations

The field equations of a system with proper boundary and initial conditions characterize the behavior of the system in terms of its variables and parameters. The dependent variables or response of the system is a function of its independent variables (input and parameters of the system). If the field equations of the scale model and its prototype are invariant under transformation Λ and Λ^{-1}, then two systems are similar [see Eq.(2.1)]. This transformation defines the scaling laws (similarity conditions) between all parameters, input, and response of the two systems. The problem of finding similarity conditions for the buckling of a column, which was analysed by dimensional analysis, is considered again (Figure 2.1). Considering the symmetric mode of deflection, the vertical reaction of spring at the middle is $k\delta$. Where δ is deflection at the middle of column. From symmetry, for half of the column $0 \leq x \leq L/2$ the reaction force is $k\delta/2$. From Simitses (1976) the differential equation and associated boundary conditions of the system are:

$$EIw_{,xx} + Pw = \frac{k\delta w}{2} \tag{2.4}$$

$$B.C. \begin{cases} w(0) = 0 \\ w_{,x}(L/2) = 0 \\ w(L/2) = \delta \end{cases}$$

For model and prototype we may write

$$E_p I_p \frac{d^2 w_p}{dx_p^2} + P_p w_p = \frac{k_p \delta_p w_p}{2} \tag{2.5}$$

$$E_m I_m \frac{d^2 w_m}{dx_m^2} + P_m w_m = \frac{k_m \delta_m w_m}{2} \tag{2.6}$$

where subscripts m and p refer to model and prototype respectively.

By defining scale factors λ_i , the variables of the prototype can be written as $x_{ip} = \lambda_{x_i} x_{im}$. The similarity conditions between model and prototype are determined by substitution of the $\lambda_{x_i} x_{im}$ into the differential equation of the prototype and by requiring that the result be the differential equation of the model, Eq.(2.5)(complete similarity).

$$(\frac{\lambda_E \lambda_I \lambda_w}{\lambda_x^2}) E_m I_m \frac{d^2 w_m}{dx_m^2} + (\lambda_p \lambda_w) P_m w_m = (\lambda_k \lambda_\delta \lambda_w) \frac{k_m \delta_m w_m}{2} \tag{2.7}$$

Eqs.(2.6) and (2.7) are the same if the terms in parentheses of Eq.(2.7) are all equal.

$$(\frac{\lambda_E \lambda_I \lambda_w}{\lambda_x^2}) = (\lambda_p \lambda_w) = (\lambda_k \lambda_\delta \lambda_w) \tag{2.8}$$

Dividing Eq.(2.8) by one of these terms, i.e. the first term ,

$$1 = \frac{\lambda_p \lambda_x^2}{\lambda_E \lambda_I} = \frac{\lambda_k \lambda_\delta \lambda_x^2}{\lambda_E \lambda_I} \tag{2.9}$$

or

$$\frac{\lambda_p \lambda_x^2}{\lambda_E \lambda_I} = 1 \qquad or \qquad \lambda_p = \lambda_x^{-2} \lambda_E \lambda_I \tag{2.10}$$

and

$$\frac{\lambda_k \lambda_\delta \lambda_x^2}{\lambda_E \lambda_I} = 1 \qquad or \qquad \lambda_k \lambda_\delta \lambda_x^2 = \lambda_E \lambda_I \tag{2.11}$$

Similarly for the boundary conditions,

$$\frac{\lambda_w}{\lambda_\delta} = 1 \qquad or \qquad \lambda_w = \lambda_\delta \tag{2.12}$$

Eqs(2.10)−(2.12) are necessary and suficient conditions for complete similarity between model and prototype. These similarity conditions define three relationship among seven unknown (λ's) . Hence we can choose four of λ's freely and find the values of the others by requiring satisfaction of the similarity conditions, Eqs.(2.10)−(2.12).

Chapter 3

PARTIAL SIMILARITY AND DISTORTED MODEL

If all the π-terms for the model and the prototype are the same, or if all similarity conditions are satisfied, the two systems are completely similar. But often complete similarity is difficult or even undesirable. The model which has some relaxations in similarity conditions is called a distorted model.

In complete similarity (in terms of π-terms) $\pi_{im} = \pi_{ip}$ for $i = 1, \cdots, N$ but in partial similarity $\pi_{im} = \pi_{ip}$ for $i = 1, \cdots, k$ where $k < N$. These relaxations in the relationship between two systems cause model behavior to be different from that of the prototype. Understanding these relaxations and their effects in model behavior can be used to modify the model test data so as to predict the behavior of the prototype.

3.1 Dimensional Analysis

In dimensional analysis, similarity of each π-term of the model with corresponding π-term of the prototype is a function of the scale factors of the variables. Since there are $m - r$ π-terms, the results will be $m - r$ functions of m scale factors. If the two systems are completely similar, the number of scale factors which can be chosen freely is equal the rank of the dimensional matrix, r , and the $m - r$ remaining scale factors are determined by solving $m - r$ similarity conditions.

complete − similarity	*partial − similarity*
$\pi_{1m}=\pi_{1p}$	$\pi_{1m}=\pi_{1p}$
$\pi_{2m}=\pi_{2p}$	$\pi_{2m}=\pi_{2p}$
$\vdots$	$\vdots$
$\pi_{km}=\pi_{1p}$	$\pi_{km}=\pi_{kp}$
$\pi_{k+1m}=\pi_{k+1p}$	$\pi_{k+1m} \neq \pi_{k+1p}$
$\vdots$	$\vdots$
$\pi_{nm}=\pi_{np}$	$\pi_{nm} \neq \pi_{np}$

For a distorted model, inequality of some π-terms causes a change in scale factors of those terms. π-terms which include these scale factors will also change. In this case, the number of unknown scale factors is greater than the number of similarity equations and additional relationships between variables are needed. Dimensional analysis cannot provide these relationships. These additional relationships between variables can be established by the governing equations of the system, such as equations of equilibrium and compatibility, kinematic relations, material behavior equations and boundary conditions. If these equations are not available, by conducting a series of experiments the effect of distortions on each term can be found while the other terms are kept constant. A sufficient amount of data should be determined from model tests so that these relationships can be understood clearly (Langhaar,1954).

3.2 Direct Use of Governing Equations

When governing equations of the system are used for establishing similarity conditions, the relationships between variables are forced by these equations. Suppose the system has m variables and similitude analysis of the governing equations of the system define n relationship among m unknown, (scale factors of these variables). If the two systems are completely similar $m-n$ scale factors can be chosen freely and the values of the other scale factors are found by using n similarity conditions. When at least one of the similarity conditions can not be satisfied, partial similarity is achieved. In this case, since each variable has different influence on the response of the system, the resulting similarity conditions have different influence. By understanding

the effect of variables and similarity conditions over desired intervals, the similarity conditions which have the least influence can be neglected without introducing significant error(Kline,1965).

Suppose we want to design a reasonable (able to test) model for a large rectangular plate. The plate is simply supported at all edges and loaded with uniform load of intensity q. Assume uniform cross section and isotropic material, the governing differential equations and boundary conditions are well known (Timoshenko, 1959)

$$\frac{d^4w}{dx^4} + 2\frac{d^4w}{dx^2dy^2} + \frac{d^4w}{dy^4} = \frac{q}{D} \tag{3.1}$$

and B.C at $x = 0, a$

$$w = 0 \tag{3.2}$$

$$M_x = -D\frac{d^2w}{dx^2} = 0 \tag{3.3}$$

and at $y = 0, b$

$$w = 0$$

$$M_y = -D\frac{d^2w}{dy^2} = 0 \tag{3.4}$$

By applying similitude theory

$$\frac{\lambda_w}{\lambda_x^4} = \frac{\lambda_w}{\lambda_x^2\lambda_y^2} = \frac{\lambda_w}{\lambda_y^4} = \frac{\lambda_q}{\lambda_D} \tag{3.5}$$

Now to find the scaling laws from Eq.(3.5), we have three choices. Dividing Eq.(3.5) by first term, yields

$$\lambda_x = \lambda_y \quad , \quad \lambda_w = \frac{\lambda_q\lambda_x^4}{\lambda_D} \tag{3.6}$$

Dividing Eq.(3.5) by the second term, yields

$$\lambda_x = \lambda_y \quad , \quad \lambda_w = \frac{\lambda_q\lambda_x^2\lambda_y^2}{\lambda_D} \tag{3.7}$$

and finally dividing Eq.(3.5) by third term

$$\lambda_x = \lambda_y \quad , \quad \lambda_w = \frac{\lambda_q\lambda_y^4}{\lambda_D} \tag{3.8}$$

To find which one of Eqs. (3.6)-(3.8) gives the best prediction for the prototype behavior, the theoretical deflections of the model are projected with each condition and compared to theoretical deflection of the prototype. For complete similarity, all three give the same results. In order to avoid impractical size for the cross section we need to choose different scale factors in the x ,y, and z directions.

Suppose $\lambda_y = C\lambda_x$ where $C > 0$. Eqs.(3.6)-(3.8) can be written as

$$\lambda_w = \frac{\lambda_q \lambda_x^4}{\lambda_D} = \bar{C}\frac{\lambda_q \lambda_x^4}{\lambda_D} \quad , \quad \bar{C} = 1 \tag{3.9}$$

$$\lambda_w = \frac{\lambda_q \lambda_x^2 \lambda_y^2}{\lambda_D} = \bar{C}\frac{\lambda_q \lambda_x^4}{\lambda_D} \quad , \quad \bar{C} = C^2 \tag{3.10}$$

$$\lambda_w = \frac{\lambda_q \lambda_y^4}{\lambda_D} = \bar{C}\frac{\lambda_q \lambda_x^4}{\lambda_D} \quad , \quad \bar{C} = C^4 \tag{3.11}$$

To find which one of Eqs.(3.9)$-$(3.11) gives the best prediction for the prototype behavior, the theoretical deflections of the model are projected with each one of these conditions, Eqs.(3.9)$-$(3.11), and compared to the theoretical deflection of the prototype.

There are three possible configurations for the prototype.

- Rectangular $\quad \frac{a}{b} > 1$
- Square $\quad \frac{a}{b} = 1$
- Inverse rectangular $\quad \frac{a}{b} < 1$

The characteristics of the model were calculated by using the given scale factors. The theoretical deflections of the model and prototype are given by the same expression. From Timoshenko (1959), the deflection is given by

$$w = \frac{16 q_0}{\pi^6 D} \sum_{m=1}^{\infty} \sum_{n=1}^{\infty} \frac{sin\frac{m\pi x}{a} sin\frac{n\pi y}{b}}{mn[(\frac{m}{a})^2 + (\frac{n}{b})^2]^2} \tag{3.12}$$

By using Eqs.(3.9)$-$(3.11) the experimental data of the model were projected to predict the deflections of the prototype. The predicted deflections of the prototype were compared to the theoretical deflections of the prototype. The result is the %

discrepancy between predicted and theoretical deflections of the prototype.

$$\%Discr. = \frac{|w_{th.} - w_{pr.}|}{w_{th.}} \times 100 \tag{3.13}$$

The % discrepancies of the prototype are calculated for different values of C (different λ_y). The different values of C imply different aspect ratios $(\frac{a}{b})$ for the model. For each C the experimental data were projected by Eqs.(3.9),(3.10), (3.11). The possibility of distortion in the y-direction for each case is investigated. In this analysis the experimental data of the model are manufactured from theoretical deflections of the model by randomly introducing a $\pm 10\%$ discrepancy. For all of these cases $\lambda_E = \lambda_\nu = \lambda_p = 1$.

Case−1:

When the prototype is a rectangular plate $(\frac{a}{b})_p > 1$, a wide range of models can be used. In this case as $C \rightarrow 10$, $(\frac{a}{b})_m$ increases, Eq.(3.11) yields excellent predictions and the % discrepancy for the prototype decreases. Similarly, when $C \rightarrow 0.01$ the % discrepancy increases. In this case, Eqs.(3.9),(3.10) are not good choices for similarity condition. In other words a rectangular plate can be replaced by another rectangular plate with different aspect ratio, where $(\frac{a}{b})_p \geq 1$ and Eq.(3.11) provides the needed similarity condition. Figures 3.2− 3.7 present the predicted and theoretical deflection of the rectangular plates for different values of C.

Case−2:

In this case the prototype is a square plate. The distortion is restricted to values of C which are close to one. It means that the model must be a rectangular with $0.83 < (\frac{a}{b})_m < 1.2$. For this case Eqs.(3.9),(3.10) yield good result. As $C \rightarrow 10$ or $C \rightarrow 0.01$ the %discrepancy increases rapidly and none of the similitude conditions, Eqs.(3.9),(3.10),and(3.11), yield acceptable results. In this case Eq.(3.11) is not a suitable similarity condition even for small distortion($(\frac{a}{b})_m \approx 1$). Figures 3.8− 3.10

show the predicted deflection of the square plates for different values of C.

Case−3:

In this case where the prototype is a rectangle with $(\frac{a}{b})_m < 1$(Inverse rectangular), Eqs.(3.9) predicted the behavior of prototype very well, when $C \rightarrow 0.01$. However as $C \rightarrow 10$ the %discrepancy increases slowly. The similarity conditions Eqs.(3.10) and (3.11) are not suitable at all, since distortion from complete similarity causes the %discrepancy to increase very fast. Figures 3.11− 3.15 demonstrate the predicted deflection of the inverse rectangular plates for different values of C.

Table 3.1: *Characteristics of the Prototypes*

prototype	a (in)	b (in)	h (in)	E ($10^6 psi$)	ν
Rectangular	6000	600	60	25	0.23
Square	6000	6000	60	25	0.23
Inverse rect.	3000	6000	60	25	0.23

Table 3.2: *Characteristics of the Models*

model	C	a (in)	λ_b	b (in)	a/b	h (in)
R1	0.01	30	2	300	0.1	0.3
R2	0.05	30	10	60	0.5	0.3
R3	0.1	30	20	30	1	0.3
R4	0.5	30	100	6	5	0.3
R5	1	30	200	3	10	0.3
R6	1.5	30	300	2	15	0.3
S1	0.1	30	20	300	0.1	0.3
S2	0.5	30	100	60	0.5	0.3
S3	1	30	200	30	1	0.3
S4	1.1	30	220	27.3	1.11	0.3
S5	1.5	30	300	20	1.5	0.3
S6	2	30	400	15	2	0.3
S7	10	30	2000	3	10	0.3
IR1	0.1	15	20	300	0.05	0.3
IR2	0.5	15	100	60	0.25	0.3
IR3	0.75	15	150	40	0.625	0.3
IR4	1	15	200	30	0.5	0.3
IR5	2	15	400	15	1	0.3
IR6	4	15	800	7.5	2	0.3
IR7	10	15	2000	3	5	0.3

R : Rectangular
S : Square
IR : Inverse rectangular

Figures 3.16– 3.18 present the discrepancies between theoretical and predicted maximum deflections of the simply supported plates as a function of C, the cross section coefficient of the model, where $0.001 < C < 10$. Each C represents a specific λ_y *or* λ_z.

Figure 3.16 shows these discrepancies for rectangular plates when different similarity conditions are used. It is observed that Eq.(3.11) can predict the maximum deflection of the model very well for a large range of C; especially for $C \geq 1$. The other conditions, Eqs.(3.9)and (3.10), have a large discrepancy for small distortion of the model.

Figure 3.17 presents the discrepancies for square plates. It is clear that none of Eqs.(3.9)–(3.11) are suitable representation of similitude for distorted models. However, for small changes in C (i.e where C is close to 1) Eq.(3.10) is reasonably accurate.

The discrepancies for inverse rectangular plates are plotted in Figure 3.18. In this case Eq.(3.9) can predict the behavior of the prototype very well as long as the configurations of model and prototype are the same.

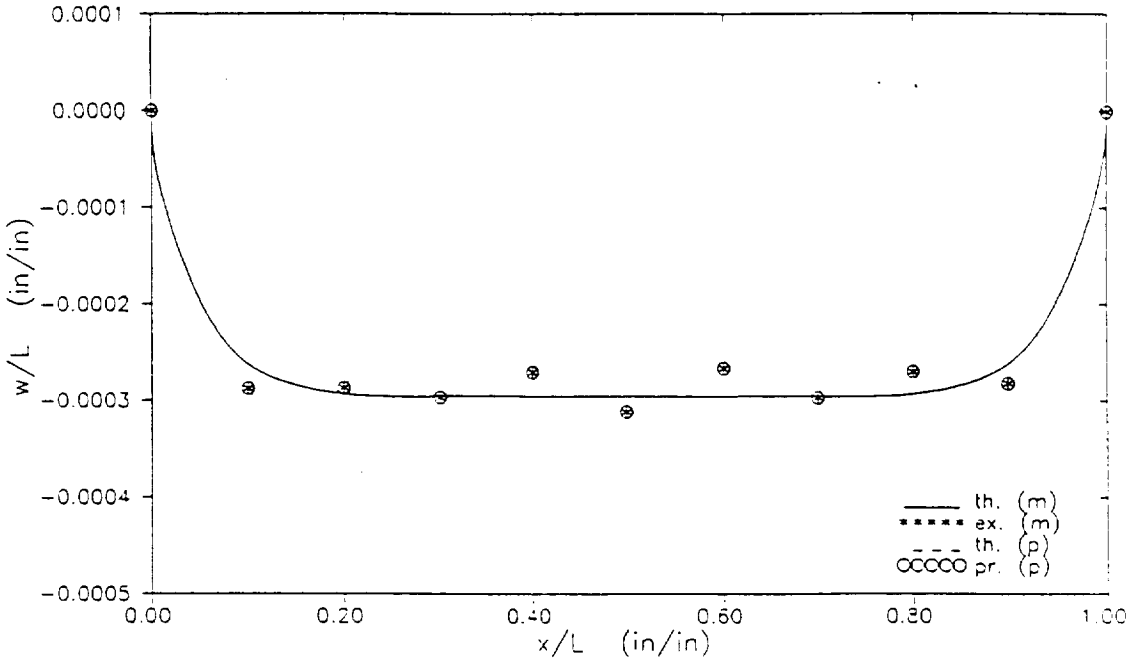

Figure 3.1: *Predicted and Theoretical Deflection of S-S Plate Complete Similarity or* $C = 1$.

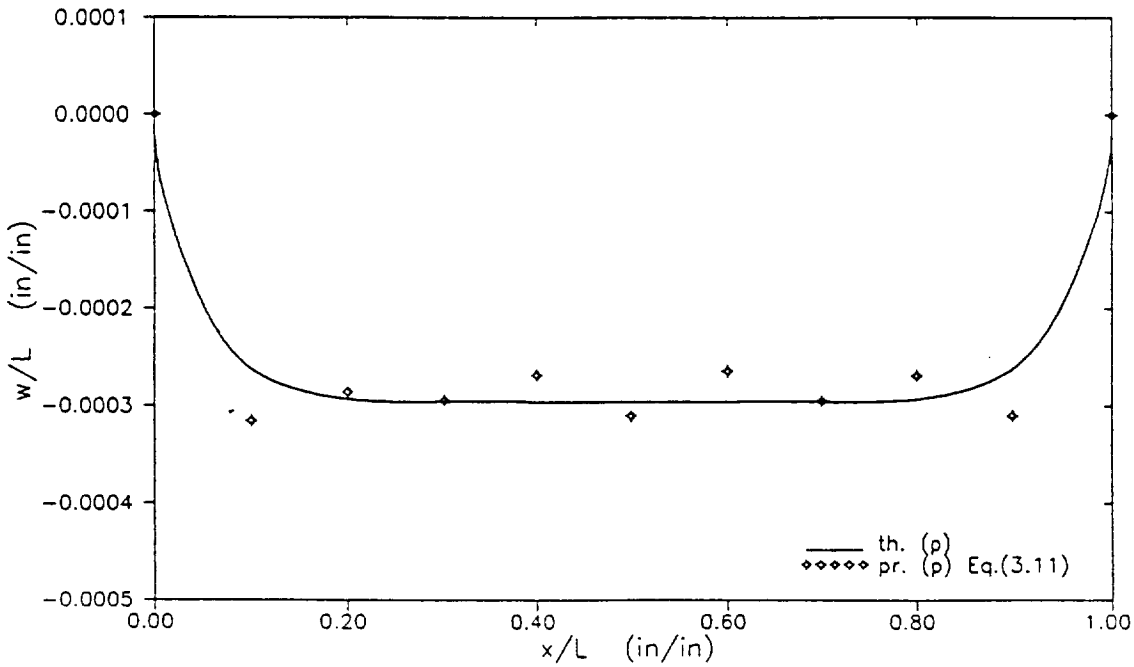

Figure 3.2: *Predicted, Eq.(3.11), and Theoretical Deflection of S-S Plate,* $(\frac{a}{b})_p > 1$ *for* $C = 1.5$.

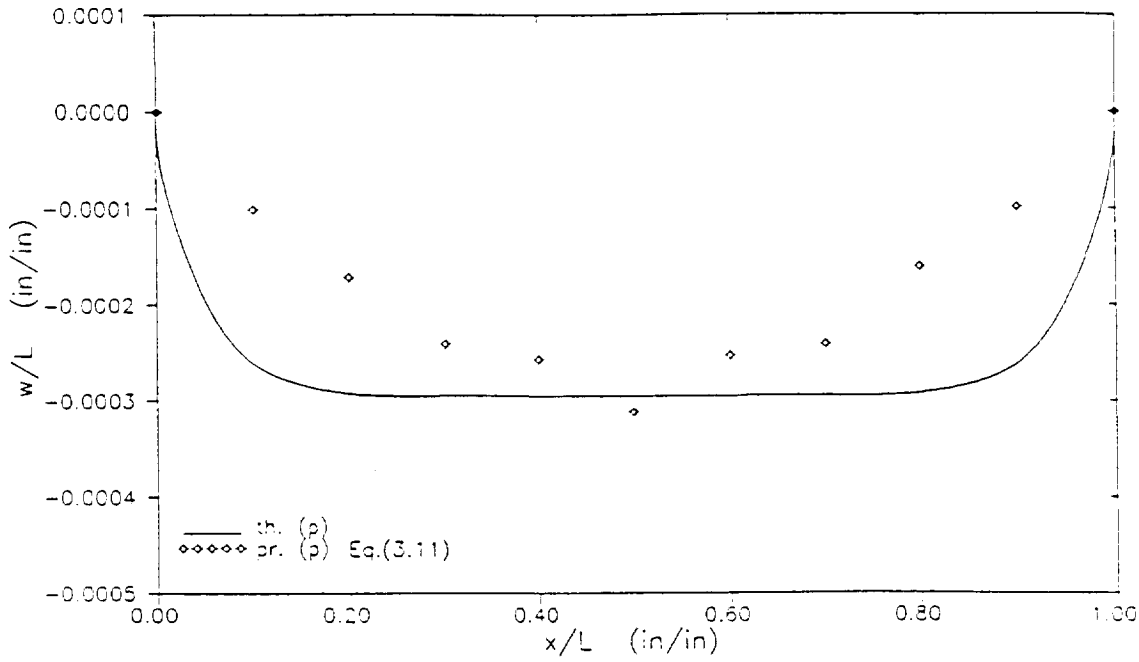

Figure 3.3: *Predicted, Eq.(3.11), and Theoretical Deflection of S-S Plate,* $(\frac{a}{b})_p > 1$ *for* $C = 0.1$.

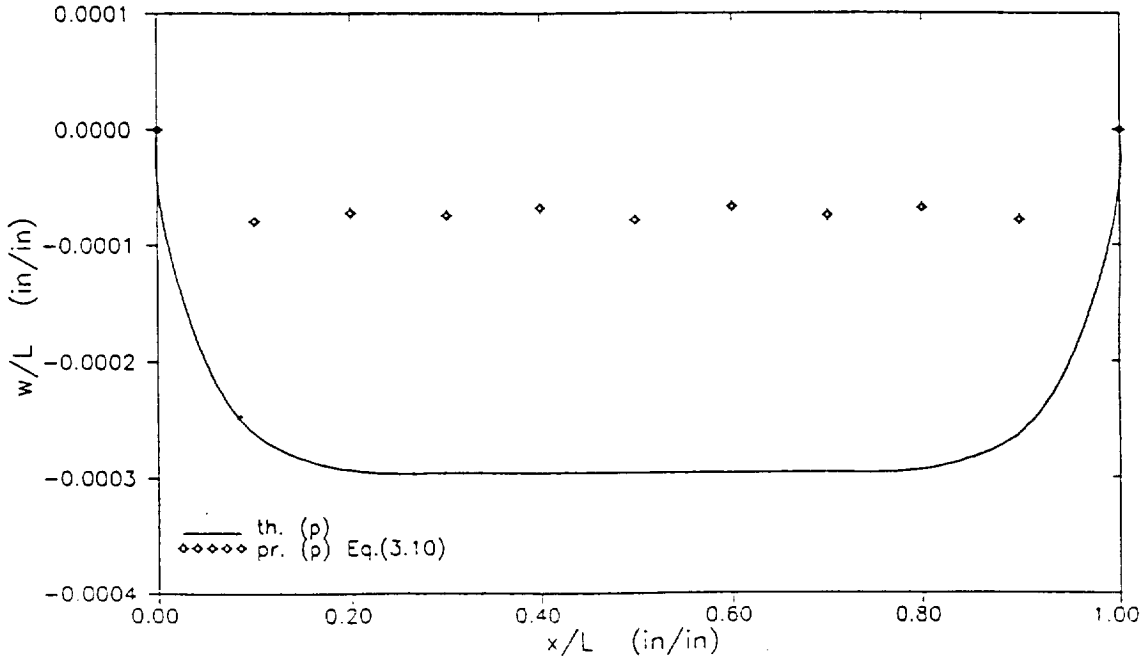

Figure 3.4: *Predicted, Eq.(3.10), and Theoretical Deflection of S-S Plate,* $(\frac{a}{b})_p > 1$ *for* $C = 2$.

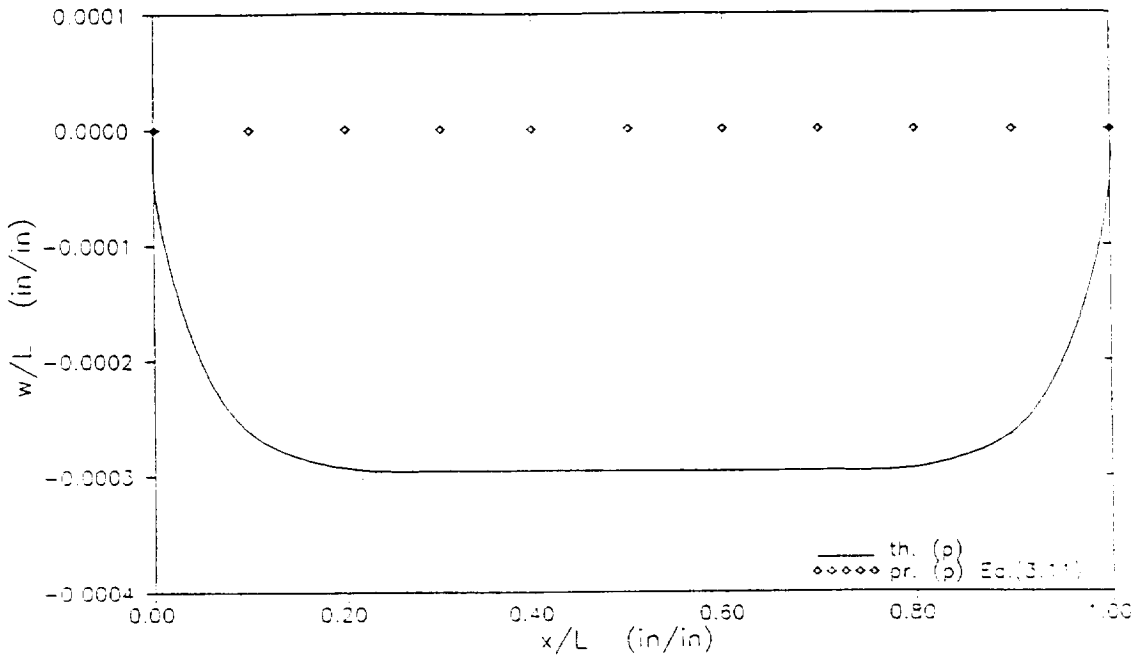

Figure 3.5: *Predicted, Eq.(3.11), and Theoretical Deflection of S-S Plate,* $(\frac{a}{b})_p > 1$ *for* $C = 0.01$.

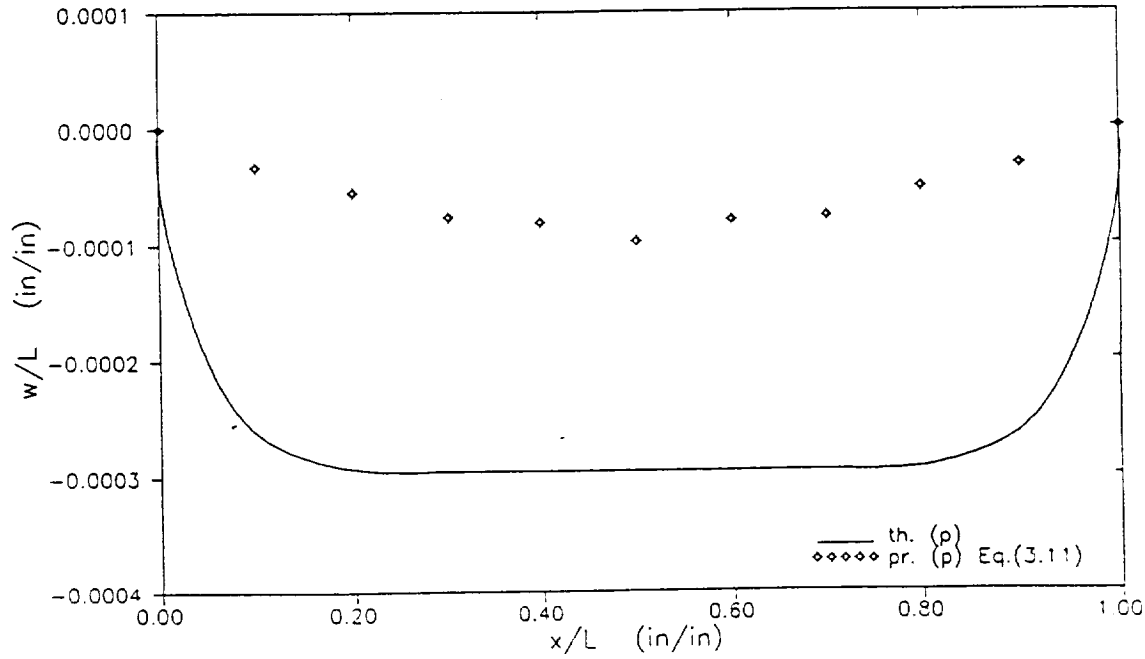

Figure 3.6: *Predicted, Eq.(3.11), and Theoretical Deflection of S-S Plate,* $(\frac{a}{b})_p > 1$ *for* $C = 0.1$.

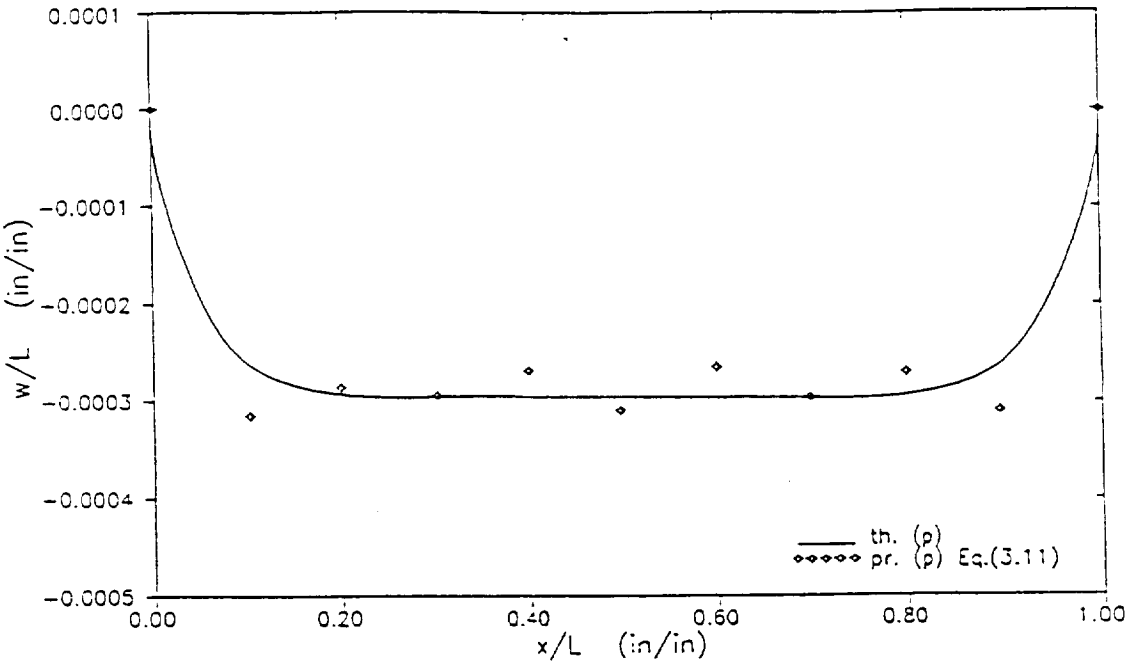

Figure 3.7: *Predicted, Eq.(3.11), and Theoretical Deflection of S-S Plate,* $(\frac{a}{b})_p > 1$ *for* $C = 2$.

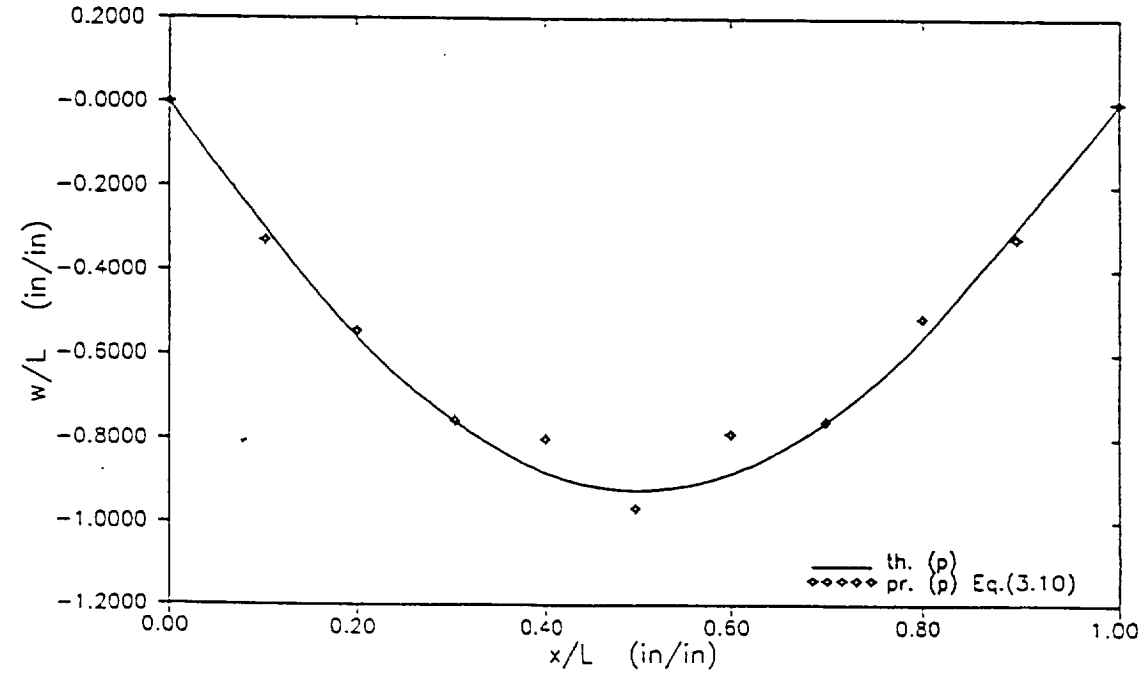

Figure 3.8: *Predicted, Eq.(3.10), and Theoretical Deflection of S-S Plate,* $(\frac{a}{b})_p = 1$ *for* $C \doteq 1.1$.

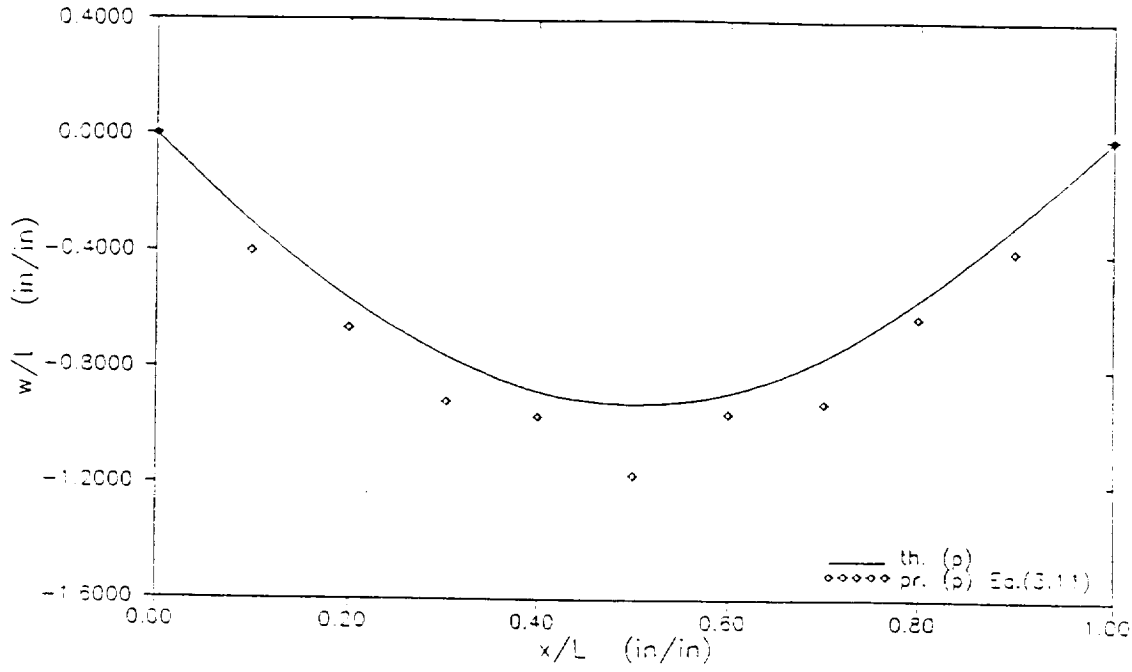

Figure 3.9: *Predicted, Eq.(3.11), and Theoretical Deflection of S-S Plate,* $(\frac{a}{b})_p = 1$ *for* $C = 1.1$.

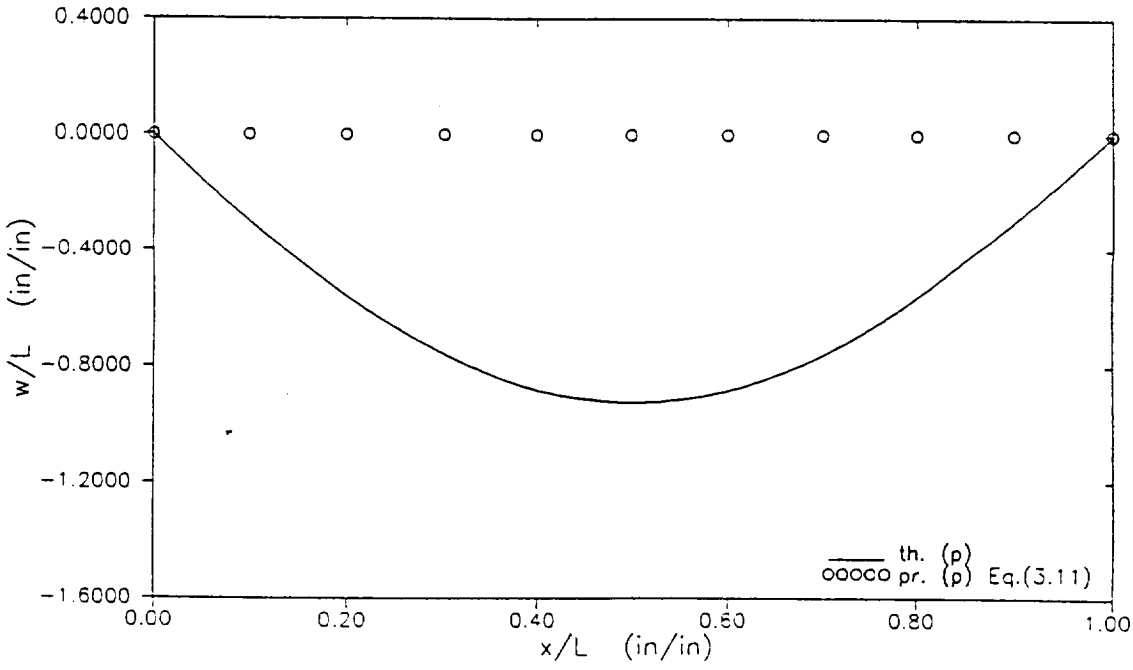

Figure 3.10: *Predicted, Eq.(3.11), and Theoretical Deflection of S-S Plate,* $(\frac{a}{b})_p = 1$ *for* $C = 0.1$.

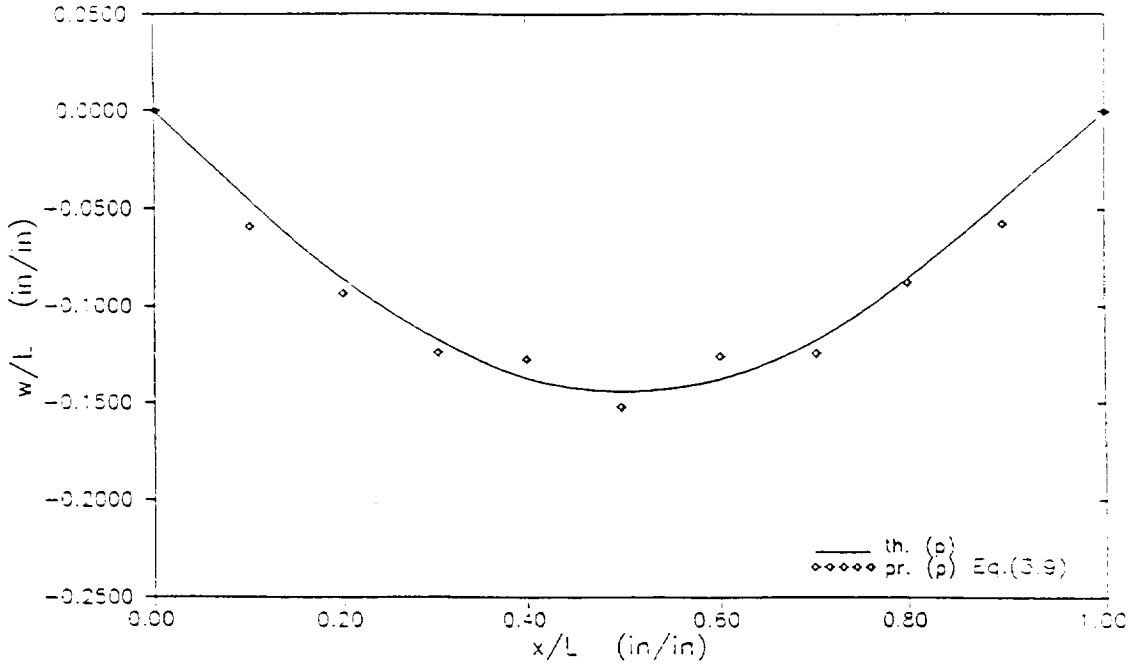

Figure 3.11: *Predicted, Eq.(3.9), and Theoretical Deflection of S-S Plate,* $(\frac{a}{b})_p < 1$ *for* $C = 0.75$.

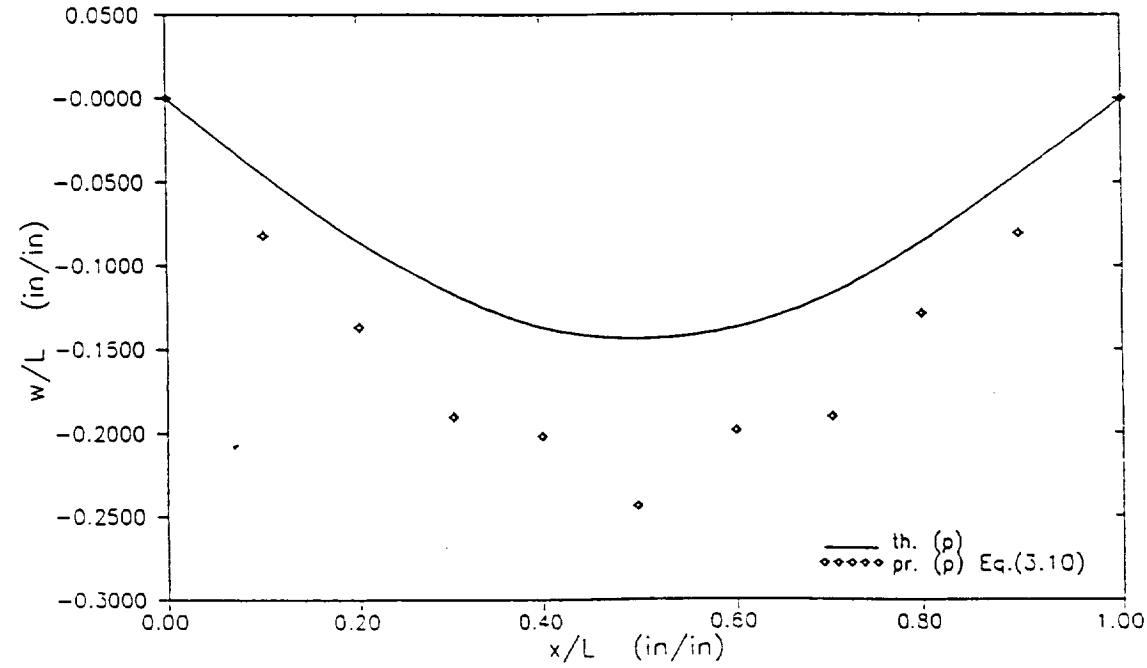

Figure 3.12: *Predicted, Eq.(3.10), and Theoretical Deflection of S-S Plate,* $(\frac{a}{b})_p < 1$ *for* $C = 2$.

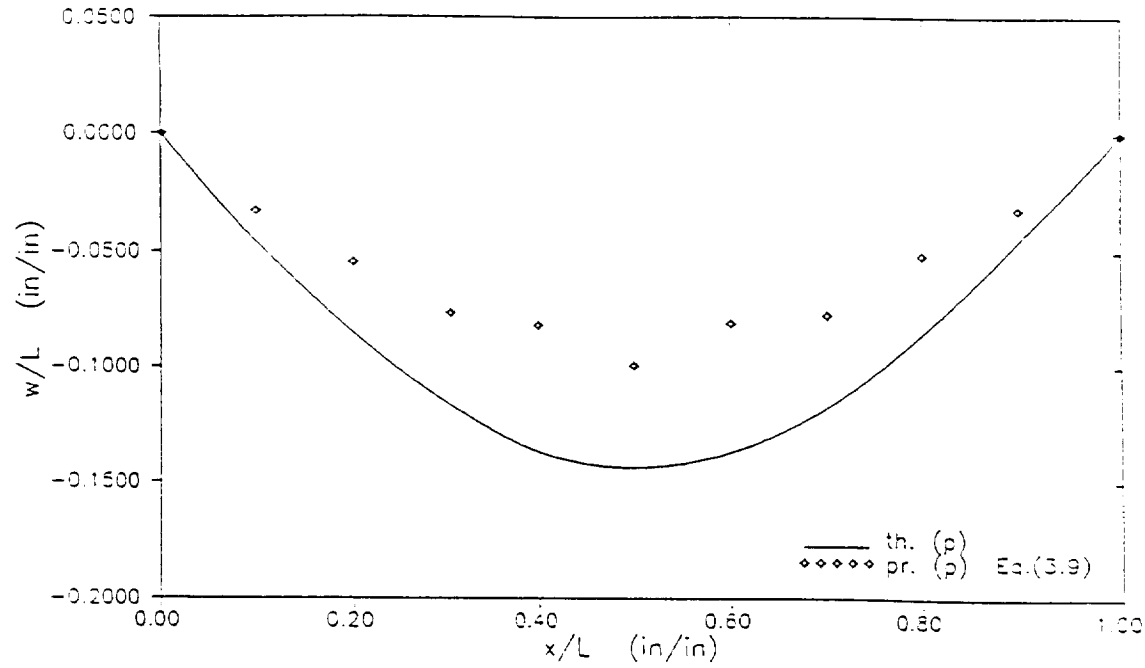

Figure 3.13: *Predicted, Eq.(3.9), and Theoretical Deflection of S-S Plate,* $(\frac{a}{b})_p < 1$ *for* $C = 4$.

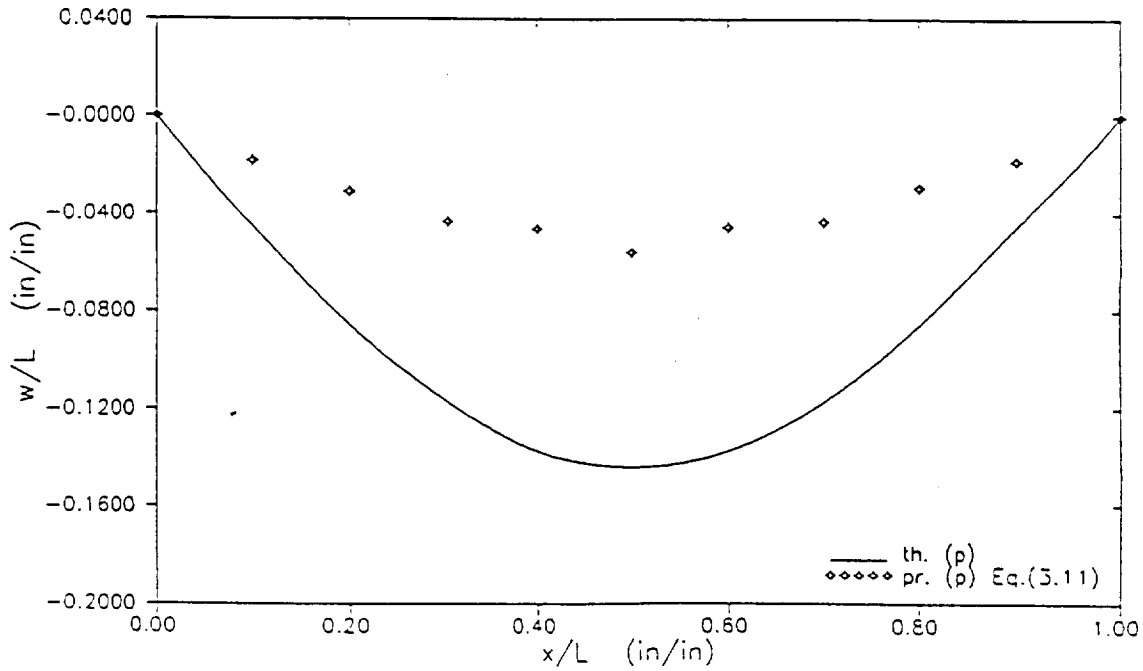

Figure 3.14: *Predicted, Eq.(3.11), and Theoretical Deflection of S-S Plate,* $(\frac{a}{b})_p < 1$ *for* $C = 0.75$.

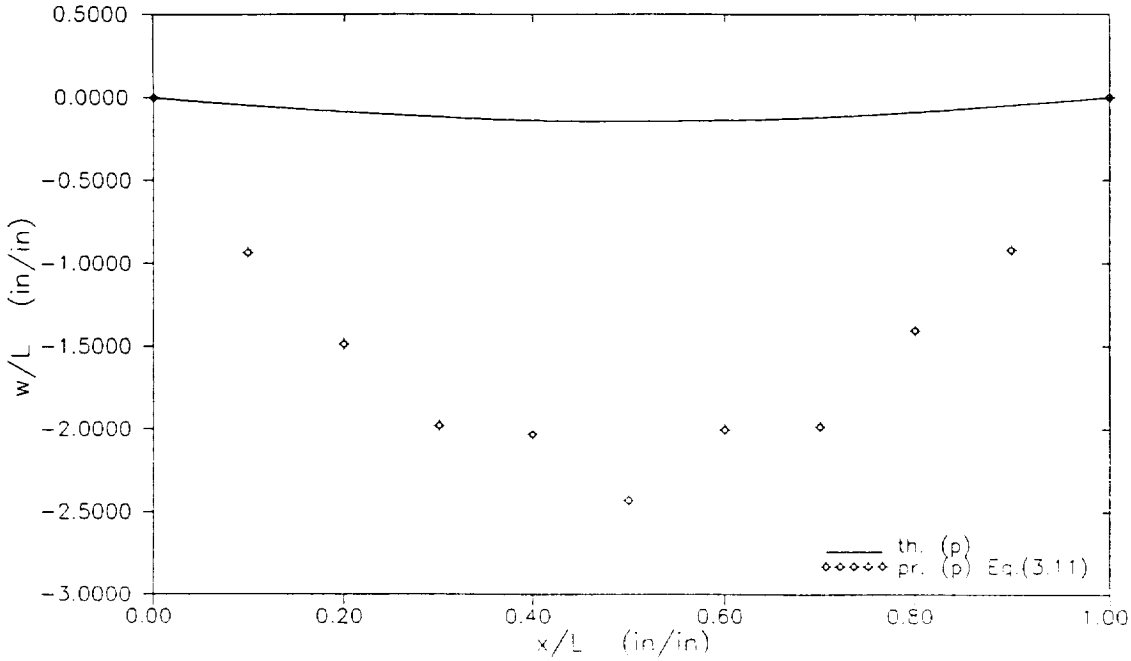

Figure 3.15: *Predicted, Eq.(3.11), and Theoretical Deflection of S-S Plate,* $(\frac{a}{b})_p < 1$ *for* $C = 4$.

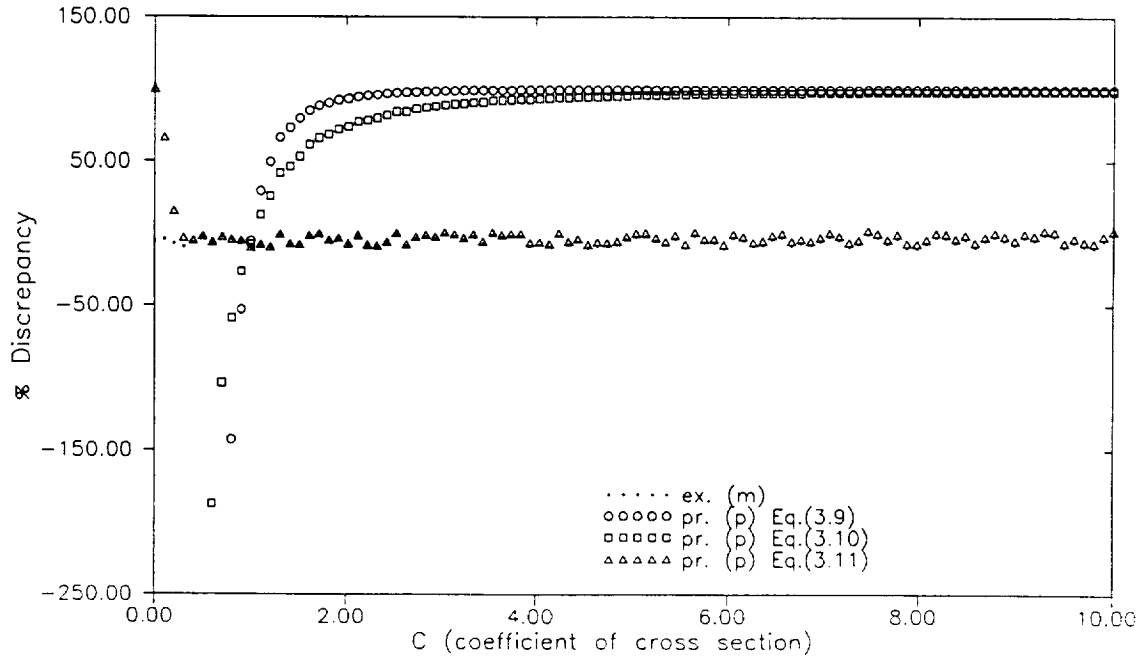

Figure 3.16: *Discrepancy Between Predicted and Theoretical Maximum Deflection of S-S Plates,* $(\frac{a}{b})_p > 1$ *for Different* C .

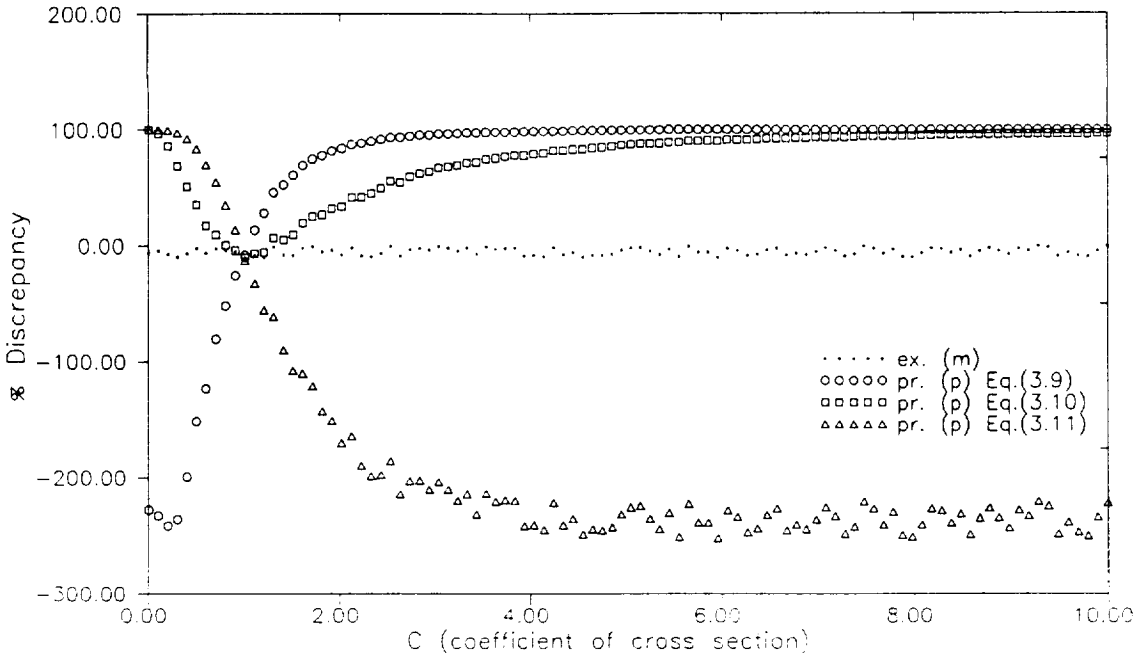

Figure 3.17: *Discrepancy Between Predicted and Theoretical Maximum Deflection of S-S Plates,* $(\frac{a}{b})_p = 1$ *for Different* C .

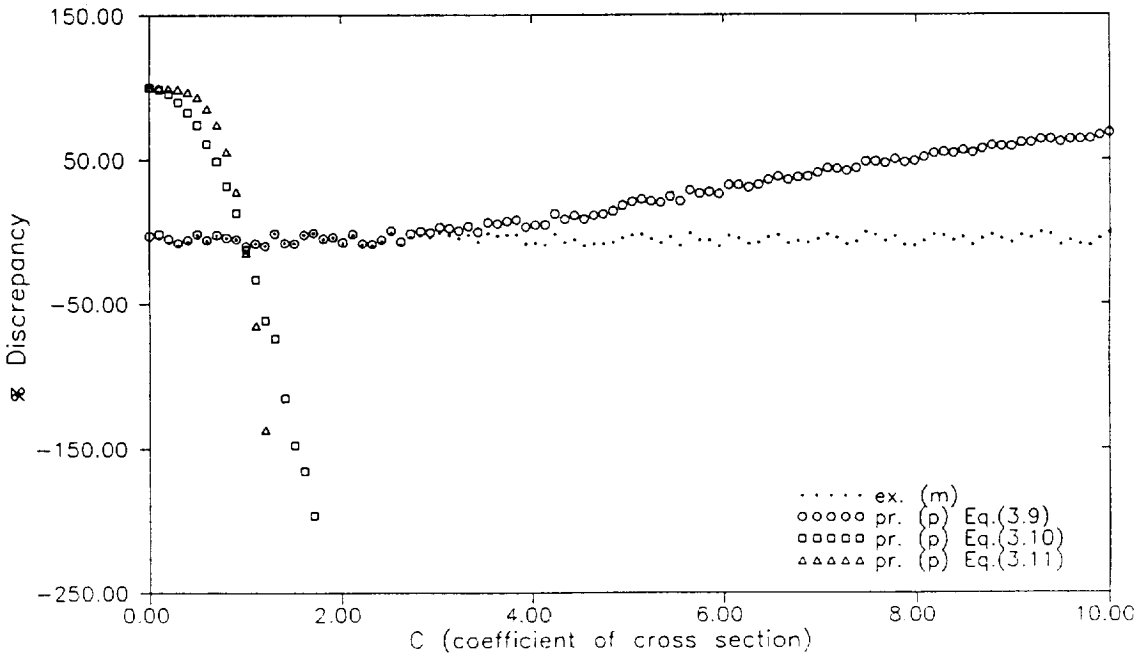

Figure 3.18: *Discrepancy Between Predicted and Theoretical Maximum Deflection of S-S Plates,* $(\frac{a}{b})_p < 1$ *for Different* C .

Chapter 4

APPLICATION TO CYLINDRICAL BENDING OF LAMINATED BEAM-PLATES

In this chapter, as an initial effort, similarity conditions are developed in order to design resonable, distorted scale models for orthotropic laminated beam-plates. Plates are subjected to transverse line loads. Later, the experimental data from 3−point tests (cylindrical bending) of the plates are used to verify the accuracy of the distorted model in order to predict the maximum deflection of the prototype.

The available experimental data is used in the following way. One of the plates is considered as prototype, the other as its scale model. Then the data of the model are projected by scaling laws in order to predict the prototype behavior. The predicted data are compared to actual experimental data of the prototype.

4.1 Similitude Analysis Based on Dimensional Analysis

Consider a cross-ply laminated plate composed of N orthotropic layers. The plate is simply supported at $x = 0, a$, free at $y = 0, b$,and subjected to a transverse line load with intensity q_0 (Fig. 4.1). The deflection of the system can be written as function of these variables ;

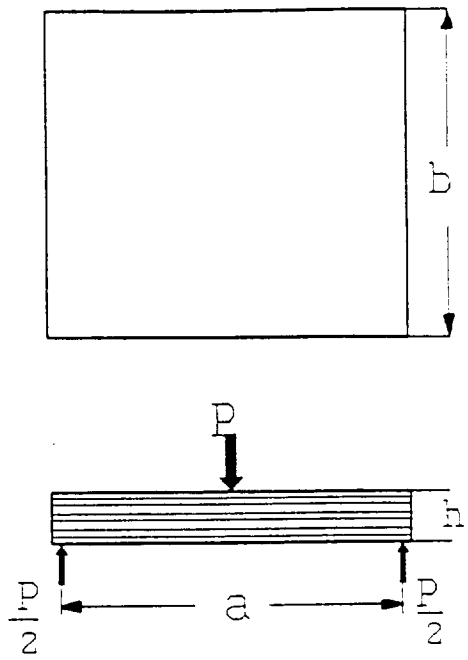

Figure 4.1: *Three Point Test of Orthotropic Beam–Plate*

variable	*dimensions*
w = *deflection*	L
a = *span*	L
E_{11} = *long. mod. of elas.*	FL^{-2}
E_{22} = *trans. mod. of elas.*	FL^{-2}
G_{12} = *modulus of rigidity*	FL^{-2}
θ = *fiber orientation*	*none*
N = *number of lamina*	*none*
h = *thickness*	L
b = *width*	L
ν_{12} = *poisson's ratio*	*none*
ν_{21} = *poisson's ratio*	*none*
q_0 = *line load*	FL^{-1}

$$\phi(w, a, E_{11}, E_{22}, G_{12}, \nu_{12}, \nu_{21}, h, b, N, \theta, q) = 0$$

The result π-terms are

$$\pi_1 = \frac{w}{a} \quad ,\pi_2 = \frac{a}{h} \quad ,\pi_3 = \frac{b}{h} \quad ,\pi_4 = \frac{G_{12}}{E_{11}} \quad ,\pi_5 = \nu_{12}$$

$$\pi_6 = \nu_{21} \quad ,\pi_7 = N \quad ,\pi_8 = \theta \quad ,\pi_9 = \frac{E_{22}}{E_{11}} \quad ,\pi_{10} = \frac{q_0}{E_{11}h}$$

where functional relation can be written as

$$\frac{w}{a} = \Phi(\frac{a}{h} \ ,\frac{b}{h} \ ,\frac{G_{12}}{E_{11}} \ ,\nu_{12} \ ,\nu_{21} \ ,N \ ,\theta \ ,\frac{E_{22}}{E_{11}} \ ,\frac{q_0}{E_{11}h})$$

complete similarity is achived if

$$\lambda_{\nu_{12}} = \lambda_{\nu_{21}} = \lambda_\theta = 1$$

$$\lambda_{E_{11}} = \lambda_{E_{22}} = \lambda_{G_{12}}$$

$$\lambda_w = \lambda_b = \lambda_h = \lambda_L$$

$$\lambda_{q_0} = \lambda_{E_{11}}\lambda_L$$

Assume the model and prototype have the same material and fiber orientation. Then from dimensional analysis (complete similarity)

$$\lambda_{\nu_{12}} = \lambda_{\nu_{21}} = \lambda_{E_{11}} = \lambda_{E_{22}} = \lambda_{G_{12}} = \lambda_\theta = 1 \tag{4.1}$$

$$\lambda_w = \lambda_a = \lambda_b = \lambda_h \tag{4.2}$$

If different scale factors are used in the x, y, z directions. Then $\lambda_a \neq \lambda_b \neq \lambda_h$ hence $\lambda_w \neq \lambda_a$ and a new relationship for λ_w must be found. Dimensional analysis cannot provide any additional information. This necessary information can be extracted from the analysis of laminated plates. Since model and its prototype both have identical governing differential equations, similarity of these equations gives the additional relationship. Thus, we have to apply similutude theory through the governing equations. For this reason in partial similarity, it is more convenient to employ similitude theory based on direct use of field equations in order to design a reasonable and acceptable distorted model.

4.2 Similitude Analysis Based on Direct Use of Governing Equations

By assuming that the displacement functions are independent of y ,or $u = u(x)$, $v = 0$, $w = w(x)$ (cylindrical bending) , from Ashton and Whitney (1970) the governing differential equations and boundary conditions are reduced to

$$\frac{d^4w}{dx^4} = \frac{qA_{11}}{A_{11}D_{11} - B_{11}^2} \tag{4.3}$$

$$\frac{d^3u}{dx^3} = \frac{B_{11}}{A_{11}}\frac{d^4w}{dx^4} \tag{4.4}$$

and the B.C.'s at $x = 0, a$ are

$$w = 0 \tag{4.5}$$

$$N_{xx} = A_{11}\frac{du}{dx} - B_{11}\frac{d^2w}{dx^2} = 0 \tag{4.6}$$

$$M_{xx} = B_{11}\frac{du}{dx} - D_{11}\frac{d^2w}{dx^2} = 0 \tag{4.7}$$

Eq.(4.3) can be written as

$$(A_{11}D_{11} - B_{11}^2)\frac{d^4w}{dx^4} = qA_{11} \tag{4.8}$$

By applying similitude theory, the resulting similarity conditions are

$$\lambda_{A_{11}}\lambda_{D_{11}}\lambda_w = \lambda_{B_{11}}^2\lambda_w = \lambda_{A_{11}}\lambda_x^4\lambda_q \tag{4.9}$$

or

$$\lambda_{A_{11}}\lambda_{D_{11}} = \lambda_{B_{11}}^2 \tag{4.10}$$

$$\lambda_w\lambda_{D_{11}} = \lambda_x^4\lambda_q \tag{4.11}$$

Similarly from Eqs.(4.4),(4.6), and (4.7) we have

$$\lambda_{A_{11}}\lambda_u\lambda_x = \lambda_w\lambda_{B_{11}} \tag{4.12}$$

$$\lambda_{B_{11}}\lambda_u\lambda_x = \lambda_w\lambda_{D_{11}} \tag{4.13}$$

The condition depicted by Eq.(4.13) does not give any new information, since it can be obtained by combining Eqs.(4.10) and (4.12). So, Eqs.(4.10)−(4.12) denote the

necessary conditions for complete similarity between scale model and its prototype. For better understanding the restrictions of Eq.(4.10), consider the definition of A_{mn},B_{mn}, and D_{mn}.

$$A_{mn} = \sum_{j=1}^{N} (\bar{Q}_{mn})_j (z_j - z_{j-1})$$

$$B_{mn} = \frac{1}{2} \sum_{j=1}^{N} (\bar{Q}_{mn})_j (z_j^2 - z_{j-1}^2)$$

$$D_{mn} = \frac{1}{3} \sum_{j=1}^{N} (\bar{Q}_{mn})_j (z_j^3 - z_{j-1}^3)$$

where z_j is the coordinate of the upper surface of the j^{th} lamina (measured from the plate reference surface). Let $z_j = c_j h$ where $-0.5 \leq c_j \leq 0.5$ and h is the total thickness ($j = 0, 1, \cdots, N$). $(\bar{Q}_{mn})_j$, the transformed stiffnesses for the j^{th} lamina is given in terms of the engineering orthotropic constants and the fiber orientation angle θ.

$$\bar{Q} = f(\theta, E_{11}, E_{22}, \nu_{12}, G_{12})$$

This allows us to express A_{mn} ,B_{mn} , D_{mn} in terms of h and functions of all $\bar{Q}$,N,and the sequence in which the plies are arranged.

$$A_{mn} = h f_a(\bar{Q}_{mn}, N)$$

$$B_{mn} = h^2 f_b(\bar{Q}_{mn}, N)$$

$$D_{mn} = h^3 f_d(\bar{Q}_{mn}, N)$$

or as scale factors

$$\lambda_{A_{mn}} = \lambda_h F_a(\bar{Q}_{mn}, N) \tag{4.14}$$

$$\lambda_{B_{mn}} = \lambda_h^2 F_b(\bar{Q}_{mn}, N) \tag{4.15}$$

$$\lambda_{D_{mn}} = \lambda_h^3 F_d(\bar{Q}_{mn}, N) \tag{4.16}$$

where $F_i = \dfrac{f_i(\bar{Q}, N)_p}{f_i(\bar{Q}, N)_m}$ $,i = a, b, d.$

Substituting Eqs.(4.14)$-$(4.16) into Eq.(4.10) we have

$$F_a(\bar{Q}_{11}, N) F_d(\bar{Q}_{11}, N) = F_b^2(\bar{Q}_{11}, N) \tag{4.17}$$

This condition, Eq.(4.17), is satisfied if the model and prototype are made of the same material with identical N and the same stacking sequence of the laminae.

4.3 Analytical Verification

In this section, the accuracy of the derived behavioral similarity conditions, Eqs.(4.10) −(4.12) is evaluated analytically, in order to determine the level of confidence that can be expected in interpreting the data from the model experiments.

Consider a cross-ply laminated E-Glass/Epoxy plate composed of 96 orthotropic layers $(0/90/0/...)_{96}$ as the prototype. We desire to find the maximum deflection of the prototype by extrapolating the pertinent values of a small scale model. The model has the same stacking sequence as the prototype but with a smaller number of layers. The prototype and its scale model have the following characteristics;

prototype $(0/90/0\ldots)_{96}$:	$a = 90$ *in*	$b = 100$ *in*	$h = 0.858$ *in*	$N = 96$
model $(0/90/0\ldots)_{16}$:	$a = 5.0$ *in*	$b = 6.139$ *in*	$h = 0.143$ *in*	$N = 16$
Scale Factors :	$\lambda_a = 18$	$\lambda_b = 16.29$	$\lambda_h = 6$	$\lambda_N = 6$

For simplification we assume that model and prototype have the same material properties ($\lambda_{E_{11}} = \lambda_{E_{22}} = \lambda_{\nu_{12}} = 1$), and $\lambda_q = \lambda_b$. By employing similarity condition Eq.(4.11), (note that $\lambda_P = \lambda_x \lambda_q$; therefore the condition becomes $\lambda_w \lambda_{D_{11}} = \lambda_x^3 \lambda_P$) the theoretical maximum deflections of the model are projected in order to predict the maximum deflections of the prototype. Figure 4.2 presents the theoretical and predicted maximum deflections of the prototype and corresponding theoretical values of the scale model. The derived scaling laws can be used with high level of accuracy in predicting the prototype behavior. Note that the model was designed by employing the free scaling factors.

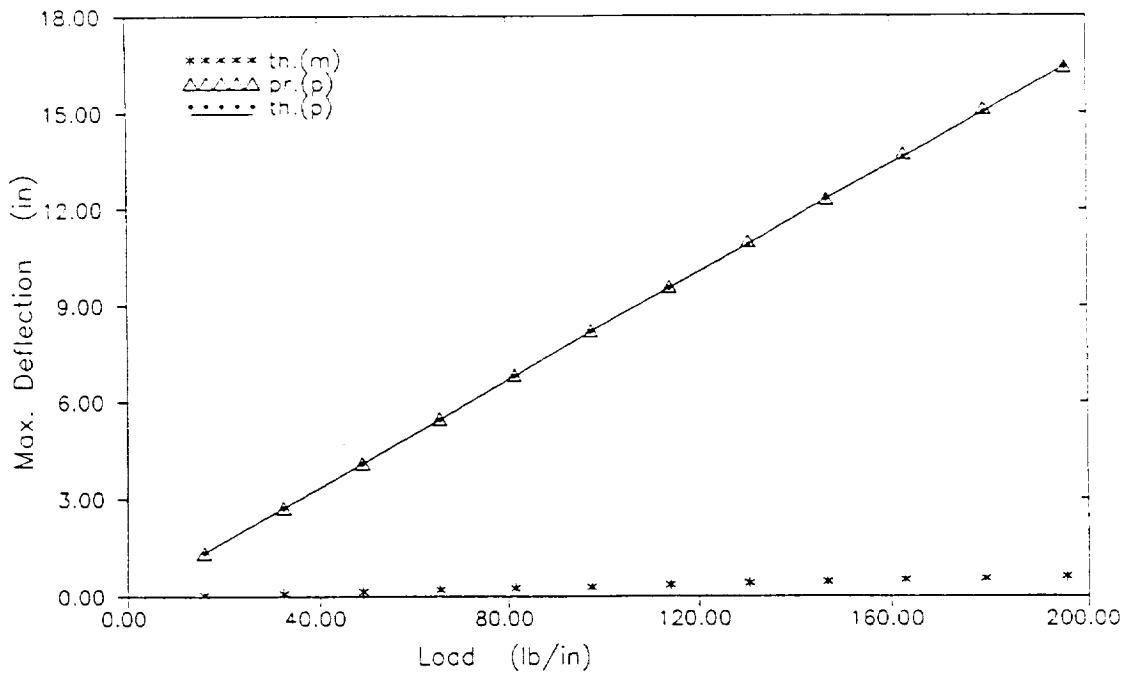

Figure 4.2: *Theoretical and Predicted Maximum Deflections of Prototype* $(0/90/0/...)_{96}$ *when model* $(0/90/0/...)_{16}$ *is used,* ($\lambda_{E_{11}} = \lambda_{E_{22}} = \lambda_{\nu_{12}} = 1$, $\lambda_a = 18$, $\lambda_b = \lambda_q = 16.92$, $\lambda_h = \lambda_N = 6$).

If the model and prototype have the same material properties then $\lambda_{\bar{Q}} = 1$. For a scale model which has equal number of plies and stacking sequence of laminae with prototype $F_i(\bar{Q}_{mn}, N) = 1$, $i = a, b, d$, and therefore $\lambda_{A_{11}}$, $\lambda_{B_{11}}$, and $\lambda_{D_{11}}$ are equal to h, h^2,and h^3 respectively. In this case the similarity condition, Eq.(4.10), is automaticly satisfied and Eqs.(4.11),(4.12) can be written as

$$\lambda_w = \lambda_x^3 \lambda_P \lambda_h{}^{-3} \tag{4.18}$$

$$\lambda_u = \lambda_w \lambda_h \lambda_x{}^{-1} \tag{4.19}$$

In general, by choosing the model material and using Eq.(4.10), the number of plies of model (N_m) can be determined. Since N_m must be an integer number, it is difficult to satisfy the Eq.(4.10) , therefore partial similarity with a distorted model is achieved.

Consider that model and prototype have the same material properties with dif-

ferent number of layers $N_m \neq N_p$. Having material properties for both systems and N_p , Eq.(4.10) determines an approximate value for N_m. Using these parameters

$$\lambda_{D_{11}} = \frac{h_p^3 . f_d(\bar{Q}, N)_p}{h_m^3 . f_d(\bar{Q}, N)_m} = c_d \lambda_h^3 \tag{4.20}$$

where $c_d = \dfrac{f_d(\bar{Q}, N)_p}{f_d(\bar{Q}, N)_m}$ and Eqs.(4.10)–(4.12) yield

$$\lambda_w = c_d^{-1} \lambda_x{}^3 \lambda_h{}^{-3} \lambda_P \tag{4.21}$$

$$\lambda_u = \frac{c_b}{c_a} \lambda_w \lambda_x^{-1} \lambda_h \tag{4.22}$$

$$\lambda_u = \frac{c_d}{c_b} \lambda_w \lambda_x^{-1} \lambda_h \tag{4.23}$$

with $c_a = \dfrac{f_a(\bar{Q}, N)_p}{f_a(\bar{Q}, N)_m}$,and $c_b = \dfrac{f_b(\bar{Q}, N)_p}{f_b(\bar{Q}, N)_m}$.

4.4 Experimental Verification

To demonstrate the use of the above analysis, the experimental data of cylindrical bending tests of 10 orthotropic plates are considered. These plates are made of E-Glass/Epoxy and Kevlar/Epoxy with different number of layers and stacking sequences of the laminae. Experimental data were provided by Professors Shive Chaturverdi and Robert Sierakowski (1991).

Table 4.1: *Characteristics of the Employed Beam−Plates*

Plate	*b(in)*	*h(in)*	*N*	*sequence*
G_1	*6.139*	*0.143*	*16*	$(0/90/0\ldots)_{16}$
G_2	*5.975*	*0.147*	*16*	$(0/90/0\ldots)_{16}$
G_3	*6.087*	*0.137*	*15*	$(0_3/90_3/0_3/90_3/0_3)$
G_4	*6.101*	*0.131*	*15*	$(0_3/90_3/0_3/90_3/0_3)$
K_5	*6.109*	*0.132*	*18*	$(0/90/0\ldots)_{18}$
K_6	*6.111*	*0.147*	*18*	$(0/90/0\ldots)_{18}$
K_7	*6.042*	*0.155*	*20*	$(0_4/90_4/0_4/90_4/0_4)$
K_8	*6.108*	*0.147*	*20*	$(0_4/90_4/0_4/90_4/0_4)$
K_9	*6.033*	*0.135*	*18*	$(0_6/90_6/0_6)$
K_{10}	*6.107*	*0.142*	*18*	$(0_6/90_6/0_6)$

G : E-Glass/Epoxy
K : Kevlar/Epoxy

Table 4.1 shows the characteristics of the plates. All plates have identical span $a = 5.0in$. In the demonstration one of these plates is considered as prototype and another one as its scale model. The derived similarity conditions, Eqs.(4.18)−(4.23), are used to project the experimental data of the model in order to predict the deflection of the prototype. By comparing the value of predicted deflection with the actual experimental deflection, the amount of discrepancy is calculated. The percentage of discrepancy is defined as

$$\%Discr. = \frac{|w_{exp.} - w_{pr.}|}{w_{exp.}} \times 100 \tag{4.24}$$

CASE – 1

In this case, plate G4 is considered as the prototype and G3 is its scale model. From the data of Table 4.1 these scale factors are calculated as;

$$\lambda_a = 1.0 \quad , \quad \lambda_b = 0.9977 \quad , \quad \lambda_h = 1.0458$$

Since the number of the plies and the stacking sequence of the laminates are identical, then λ_w is [Eq.(4.18)]

$$\lambda_w = \lambda_a{}^3 \lambda_q \lambda_h{}^{-3} \tag{4.25}$$

Since λ_a and λ_h are known, Eq.(4.25) relates λ_w and λ_q. By choosing λ_q , the corresponding λ_w is determined. λ_q must be chosen based on elastic limit of the model and the prototype. In this case, since both the model and prototype are made of the same material, λ_q can be expressed as a function of size scales (λ_a, λ_b, or λ_h) and $\lambda_{E_{11}}$. For different nondimensionalized loads, λ_q can be written as

$$\lambda_q = \lambda_{E_{11}} \lambda_a = 1 \tag{4.26}$$

$$\lambda_q = \lambda_{E_{11}} \lambda_b = \lambda_b \tag{4.27}$$

$$\lambda_q = \lambda_{E_{11}} \lambda_h = \lambda_h \tag{4.28}$$

Figures 4.3 and 4.4 show the theoretical, predicted and experimental values of the maximum deflection of the prototype G4 and its model G3 as functions of load. As shown the model can predict the maximum deflections of the prototype with very high accuracy. For clearer presentation of the results, the % discrepancy between the model (experimental and theory) and its prototype (predicted and experimental , predicted and theoretical) are shown in Fig 4.5 and 4.6. The % discrepancy between predicted and experimental deflections of the prototype are less than 6%. This indicates an excellent prediction. The predicted data match very well with experimental and theoretical deflections of the prototype.

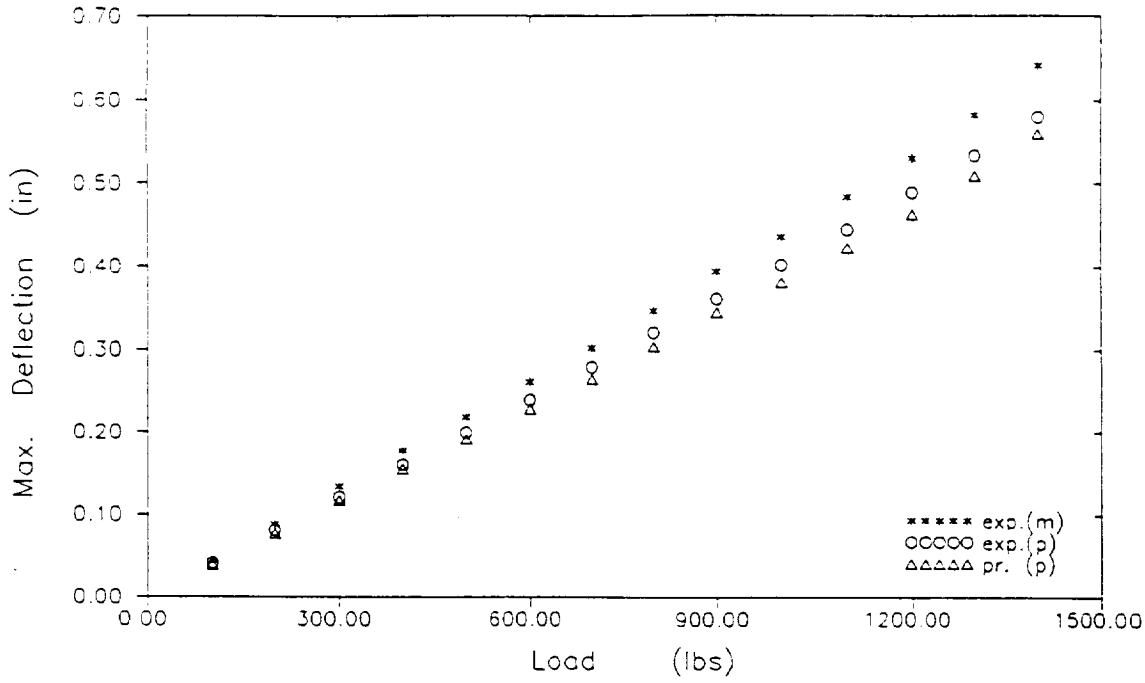

Figure 4.3: *Predicted and Actual Test Results of E-Glass/Epoxy Plate G3* $(0_3/90_3/0_3/90_3/0_3)$ *and its Model G4* $(0_3/90_3/0_3/90_3/0_3)$.

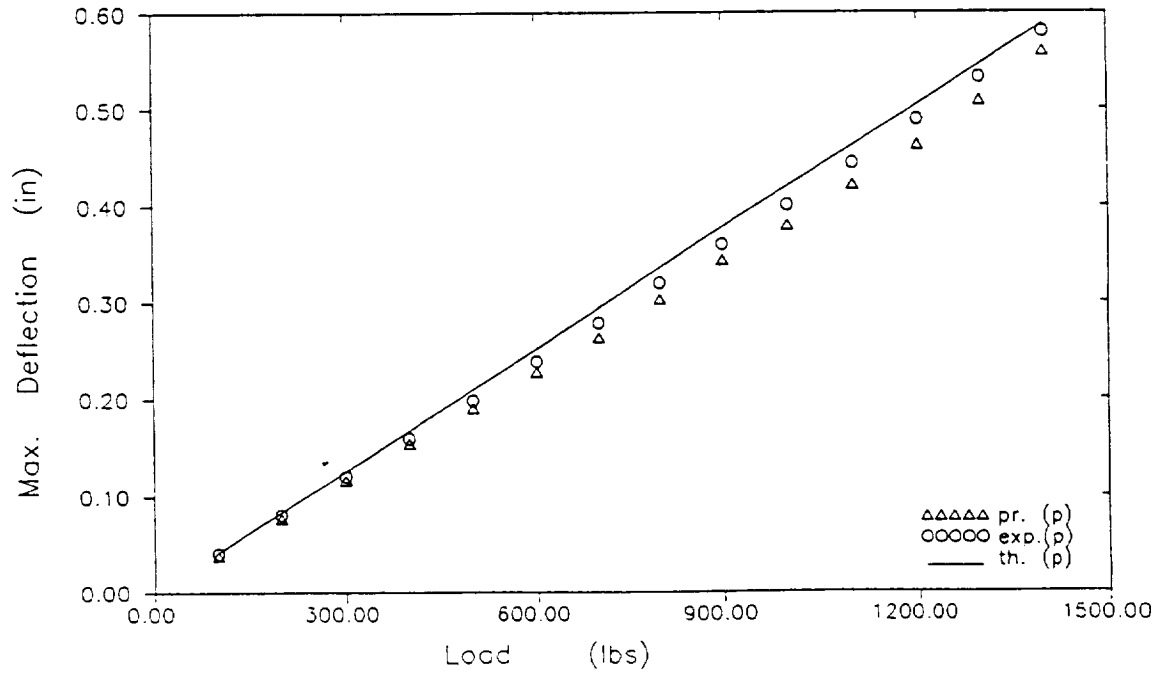

Figure 4.4: *Theoretical, Predicted, and Actual Test Results of Prototype G3* $(0_3/90_3/0_3/90_3/0_3)$ *When G4* $(0_3/90_3/0_3/90_3/0_3)$ *Is Used as Model.*

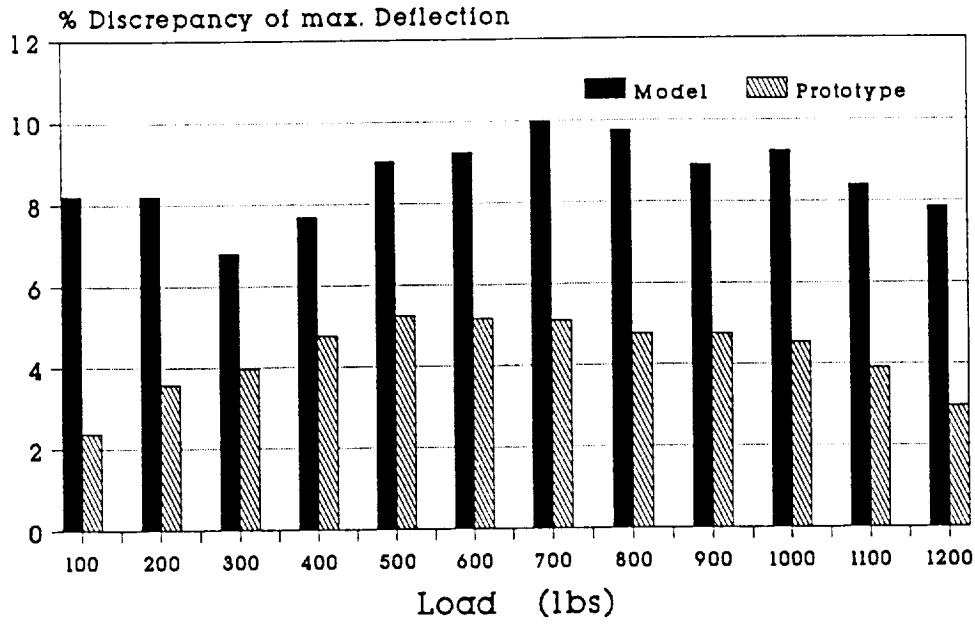

Figure 4.5: *%Discrepancy of Theory and Actual Test Results of Prototype G3* $(0_3/90_3/0_3/90_3/0_3)$ *and its Model G4* $(0_3/90_3/0_3/90_3/0_3)$.

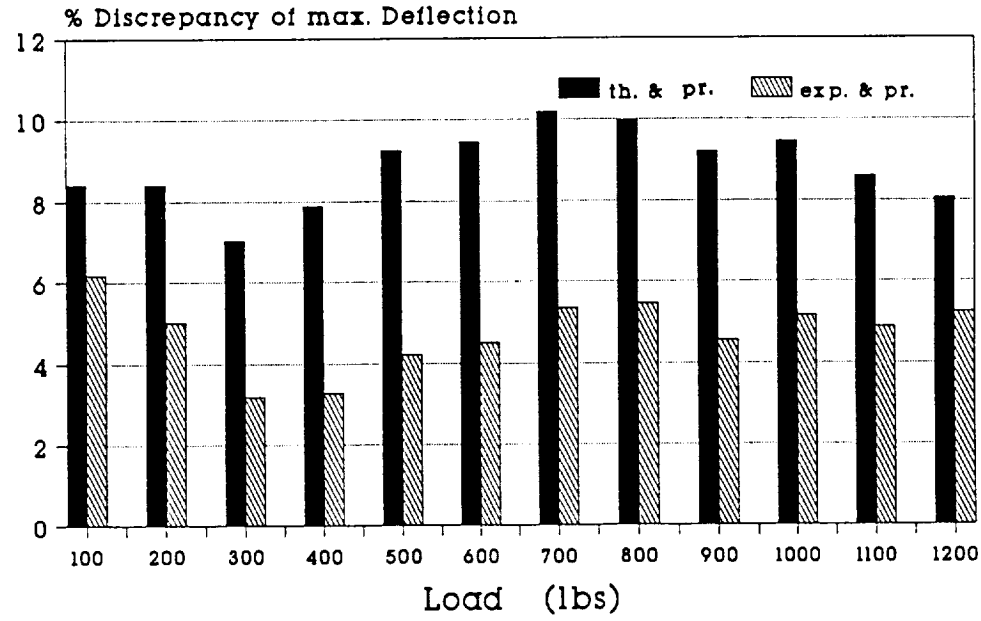

Figure 4.6: *%Discrepancy for Prototype G3* $(0_3/90_3/0_3/90_3/0_3)$ *When Model G4* $(0_3/90_3/0_3/90_3/0_3)$ *is Used.*

CASE – 2

In this case, two Glass/Epoxy Plates G2 and G4 are considered as the prototype and its scale model respectively. From the data of Table 4.1, the scale factors are calculated as;

$$\lambda_a = 1.0 \quad , \quad \lambda_b = 0.9793 \quad , \quad \lambda_h = 1.1221$$

The prototype and model have different stacking sequence and number of the laminae ($\lambda_N \neq 1$). Since the number of plies and their stacking sequence are not identical, then λ_w is

$$\lambda_w = c_d \lambda_a{}^3 \lambda_h{}^{-3} \lambda_q$$

where

$$c_d = \frac{(512Q_{11} + 512Q_{22})}{(668.25Q_{11} + 175.5Q_{22})} \lambda_N{}^{-3}$$

The experimental, predicted and theoretical values of the maximum deflection of the prototype and the experimental data of the model are presented in Figures 4.7 and 4.8 . The predicted values of maximum deflection of the prototype are in excellent agreement with its experimental data. Figures 4.9 and 4.10 show the % discrepancy between the model and prototype. The % discrepancy between predicted and experimental results of the prototype are less than 5% while this value is $10\% - 15\%$ for the theoretical and experimental data of the prototype, and $9\% - 12\%$ for theoretical and predicted data of the prototype.

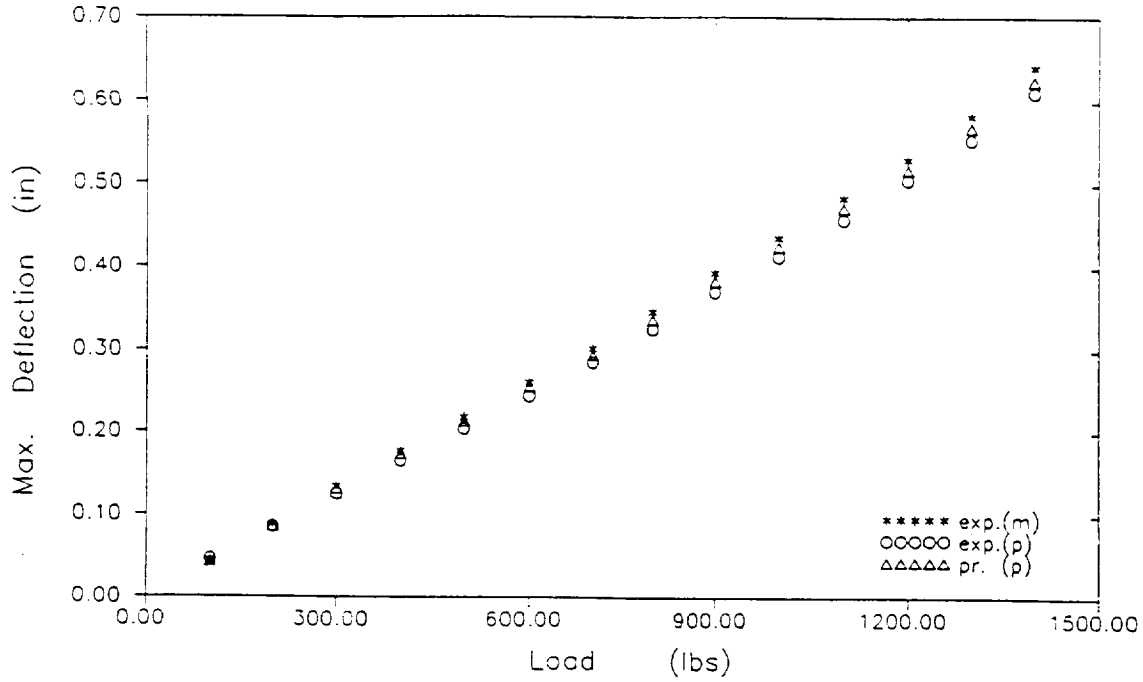

Figure 4.7: *Predicted and Actual Test Results of E-Glass/Epoxy Plate G2* $(0/90/0/...)_{16}$ *and its Model G4* $(0_3/90_3/0_3/90_3/0_3)$.

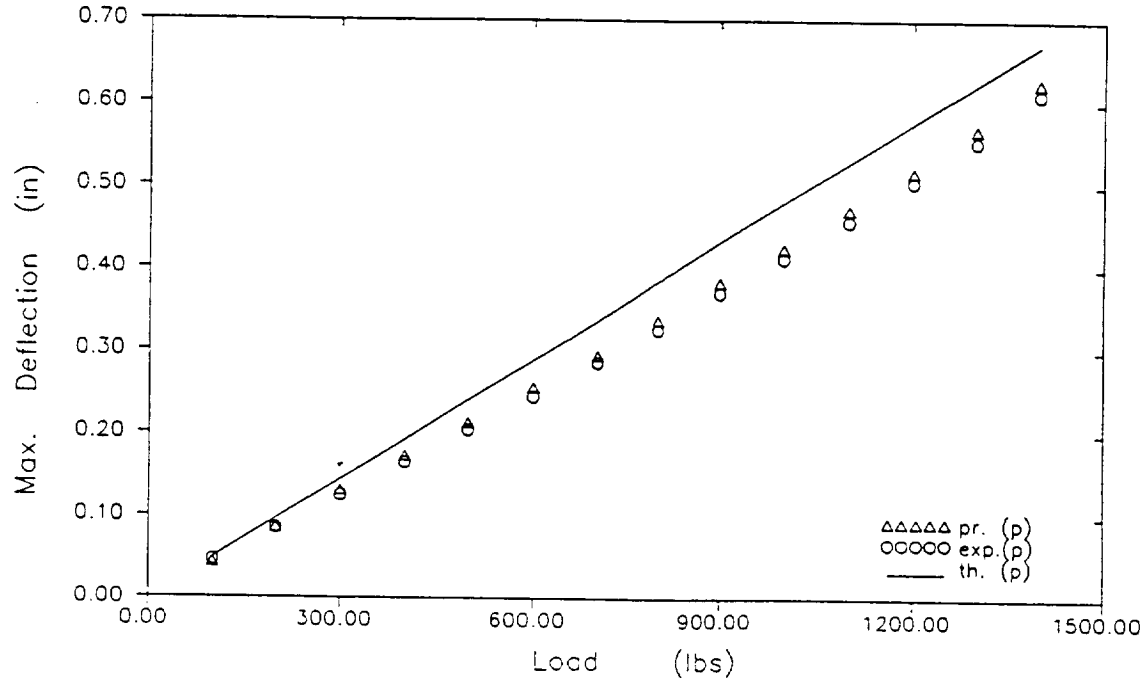

Figure 4.8: *Theoretical, Predicted, and Actual Test Result of Prototype G2* $(0/90/0/...)_{16}$, *By Using Model G4* $(0_3/90_3/0_3/90_3/0_3)$.

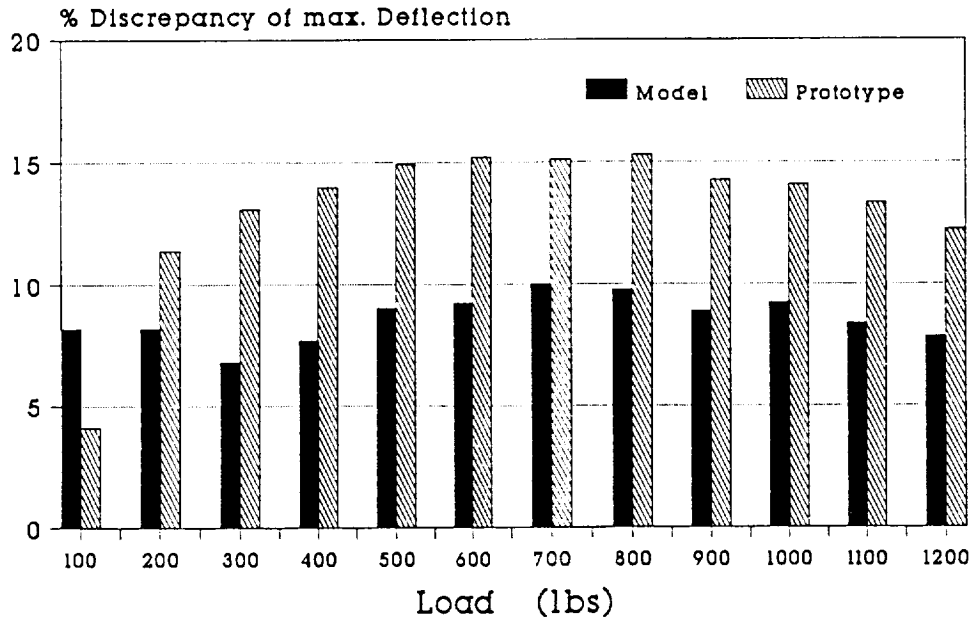

Figure 4.9: *%Discrepancy of Theory and Actual Test Results of Prototype G2* $(0/90/0/...)_{16}$ *and its Model G4* $(0_3/90_3/0_3/90_3/0_3)$.

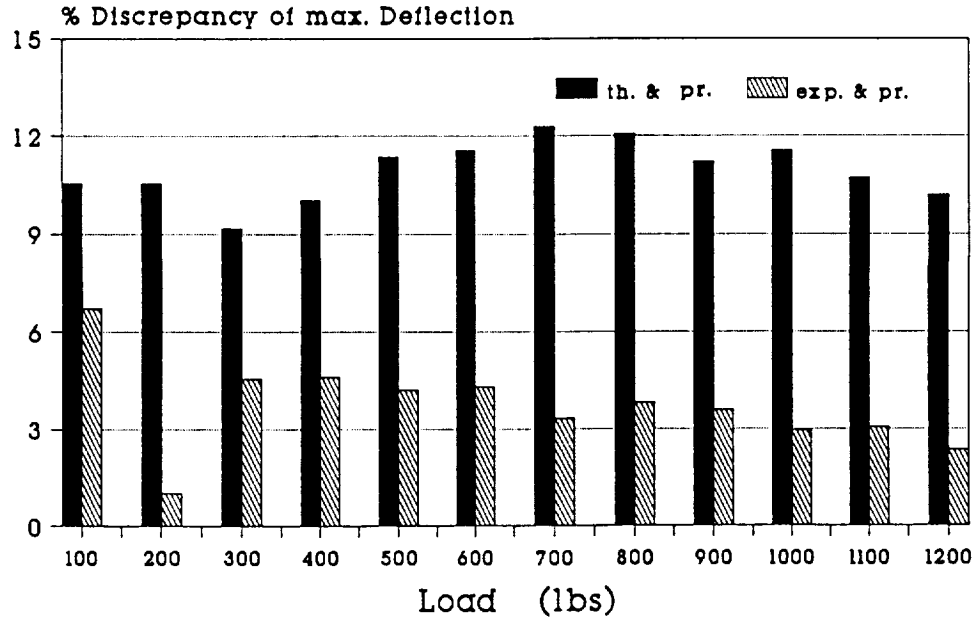

Figure 4.10: *%Discrepancy for Prototype G2* $(0/90/0/...)_{16}$ *When G4* $(0_3/90_3/0_3/90_3/0_3)$ *is Used as Model.*

CASE – 3

In this case, the E-Glass/Epoxy plate G4 is chosen as model which is used to predict the behavior of a Kevlar/Epoxy plate. The plate K7 is the prototype.

From the data of Table 4.1 , the scale factors are calculated as;

$$\lambda_a = 1.0 \quad , \quad \lambda_b = 0.9903 \quad , \quad \lambda_h = 1.1832$$

The prototype and its model have different numbers of plies with different stacking sequences. Similar to Case – 2, the λ_w is,

$$\lambda_w = c_d \lambda_a{}^3 \lambda_h{}^{-3} \lambda_q$$

where

$$c_d = \frac{(1584 Q_{11} + 416 Q_{22})}{(668.25 Q_{11} + 175.5 Q_{22})} \lambda_N{}^{-3}$$

Figures 4.11 and 4.12 show the predicted and actual experimental deflections for different loads. The discrepancies for both the model and prototype are shown in Figures 4.13 and 4.14. The discrepancies between theory and experiment, and experiment and predicted for the prototype are very high (more than 35%). But the differences between theoretical and predicted data are less than 11%. Comparing the values of these two discrepancies (experiment and theory, and experiment and predicted) of the prototype, they are in good agreement.

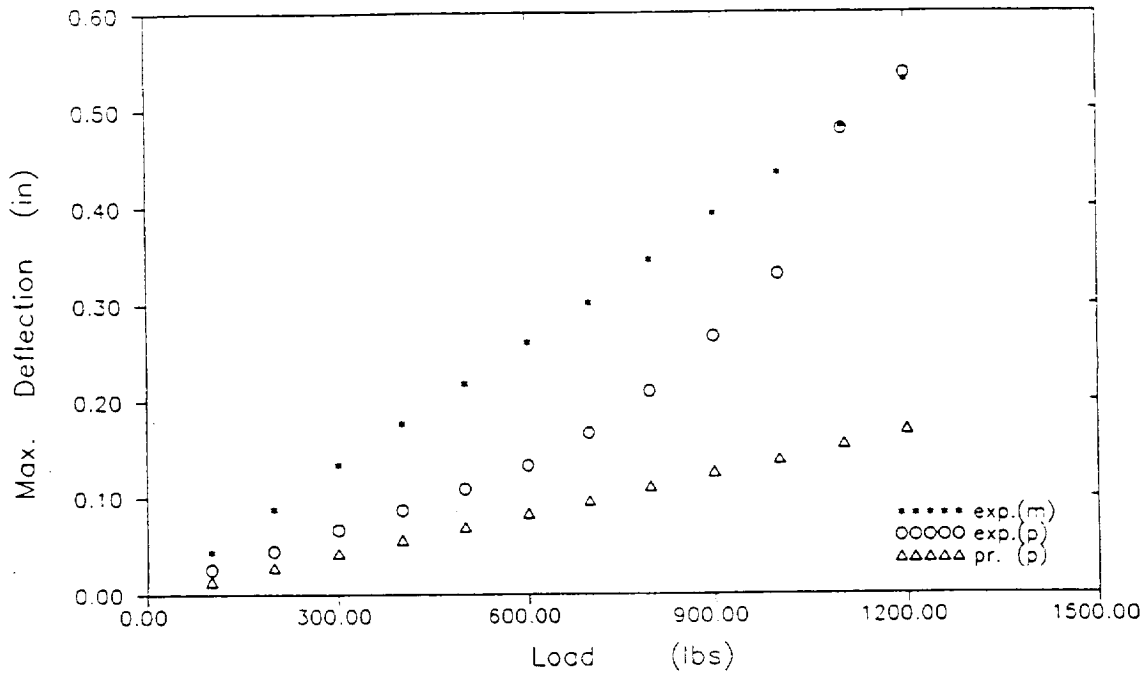

Figure 4.11: *Predicted and Actual Test Results of Kevlar/Epoxy Plate K7* $(0_4/90_4/0_4/90_4/0_4)$ *and its Model G4* $(0_3/90_3/0_3/90_3/0_3)$.

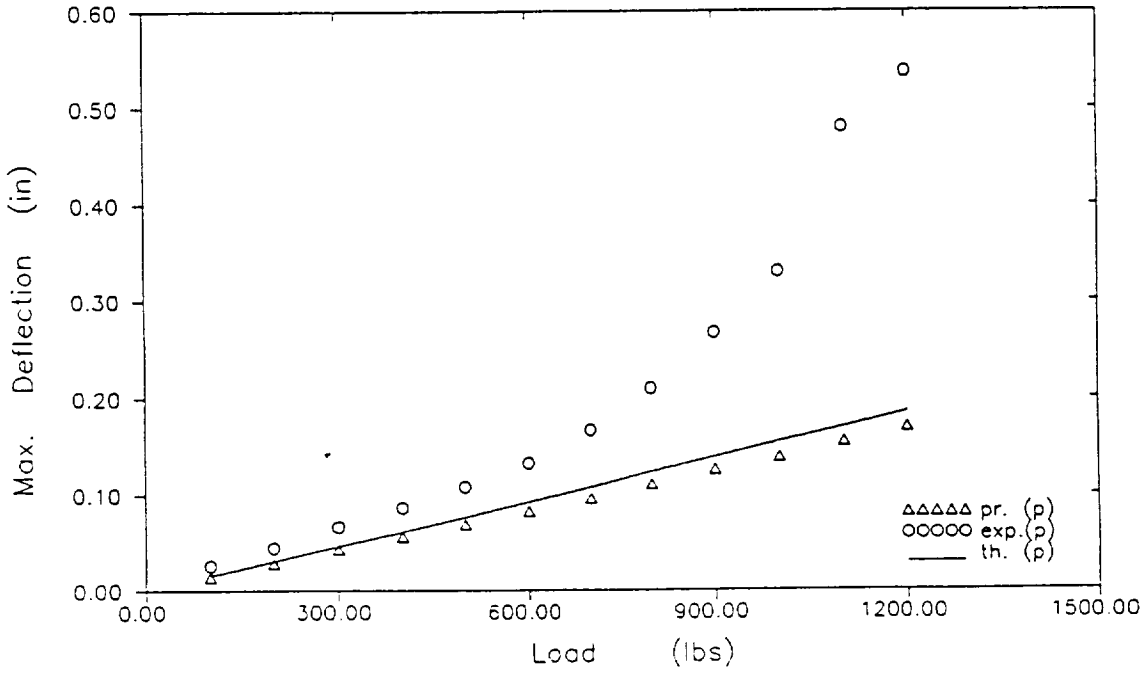

Figure 4.12: *Theoretical, Predicted, and Actual Test Result of Prototype K7* $(0_4/90_4/0_4/90_4/0_4)$ *By Using Model G4* $(0_3/90_3/0_3/90_3/0_3)$.

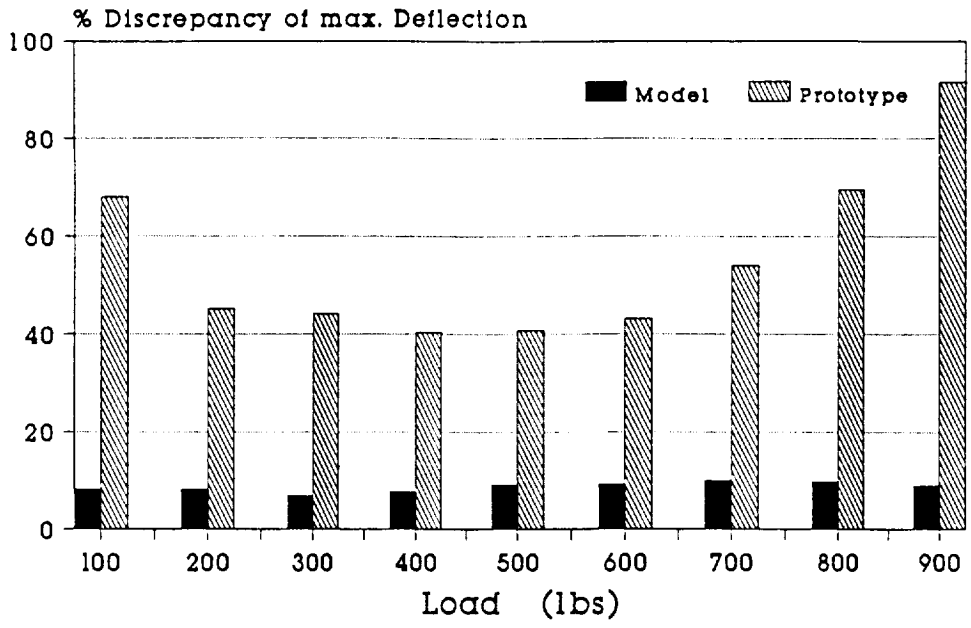

Figure 4.13: *%Discrepancy of Theory and Actual Test Results of Kevlar/Epoxy Plate K7* $(0_4/90_4/0_4/90_4/0_4)$ *and its Model G4* $(0_3/90_3/0_3/90_3/0_3)$.

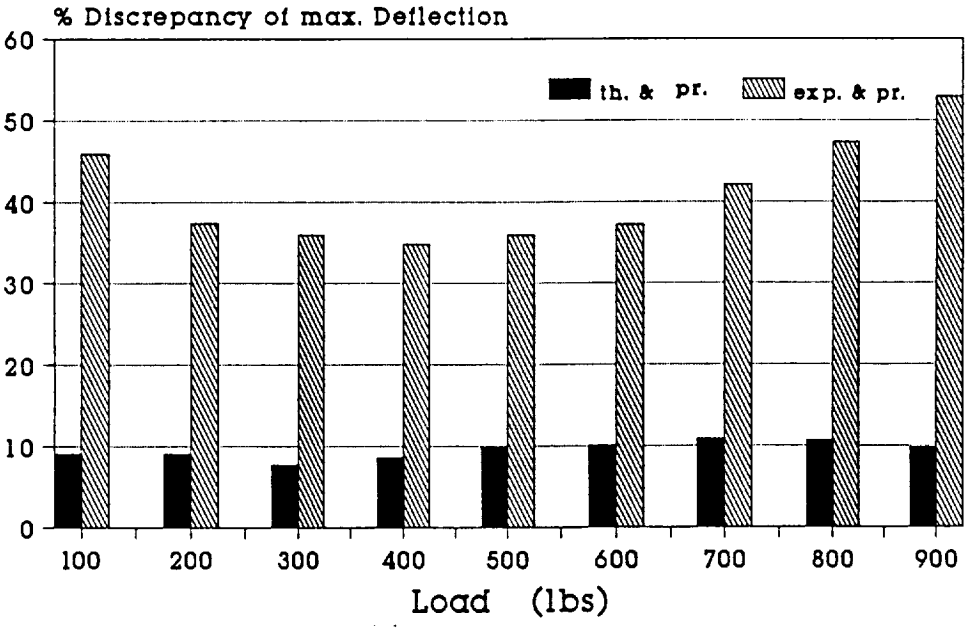

Figure 4.14: *%Discrepancy for Prototype K7* $(0_4/90_4/0_4/90_4/0_4)$ *When Model G4* $(0_3/90_3/0_3/90_3/0_3)$ *is Used.*

CASE – 4

In this case, the model and prototype have different stacking sequences of the laminae and $\lambda_N \neq 1$. Plate K8 is the prototype and K6 is chosen as its scale model. From the data of Table 4.1 , the scale factors are calculated as;

$$\lambda_a = 1.0 \quad , \quad \lambda_b = 0.9995 \quad , \quad \lambda_h = 1.0$$

Since the number of plies and the stacking sequence of the laminates are not identical, then λ_w is

$$\lambda_w = c_d \lambda_a{}^3 \lambda_h{}^{-3} \lambda_q$$

where

$$c_d = \frac{(1584Q_{11} + 416Q_{22})}{(729Q_{11} + 729Q_{22})} \lambda_N{}^{-3}$$

Similar to other cases, Figures 4.15 and 4.16 show the maximum deflections. The predicted results of the prototype match very well with the experimental data, especially for $P \geq 600lbs$. Beyond this point the theory cannot predict the actual behavior of the prototype (possibly due to fiber or ply failure). Figures 4.17 and 4.18, which present the % discrepancies for the model and prototype, show this agreement between experimental and predicted data more clearly. As the load increases the discrepancy between theory and experiment for both model and prototype increase rapidly, while the discrepancies between predicted and experimental do not change significantly.

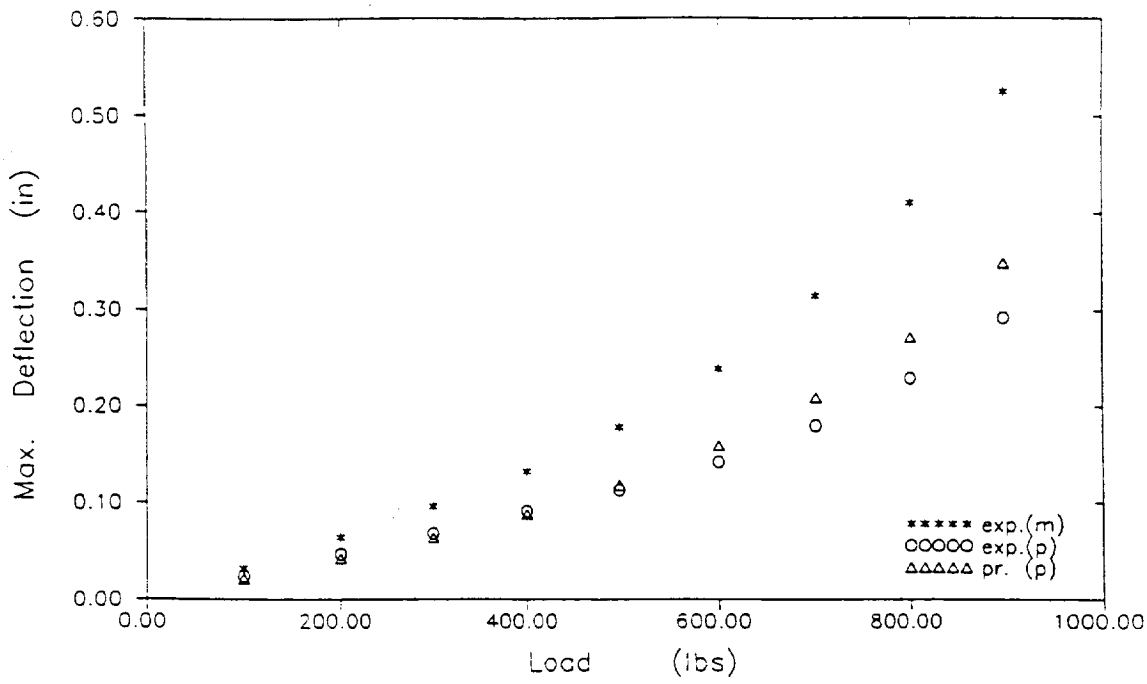

Figure 4.15: *Predicted and Actual Test Results of Kevlar/Epoxy Plate K8* $(0_4/90_4/0_4/90_4/0_4)$ *and its Model K6* $(0/90/0/...)_{18}$

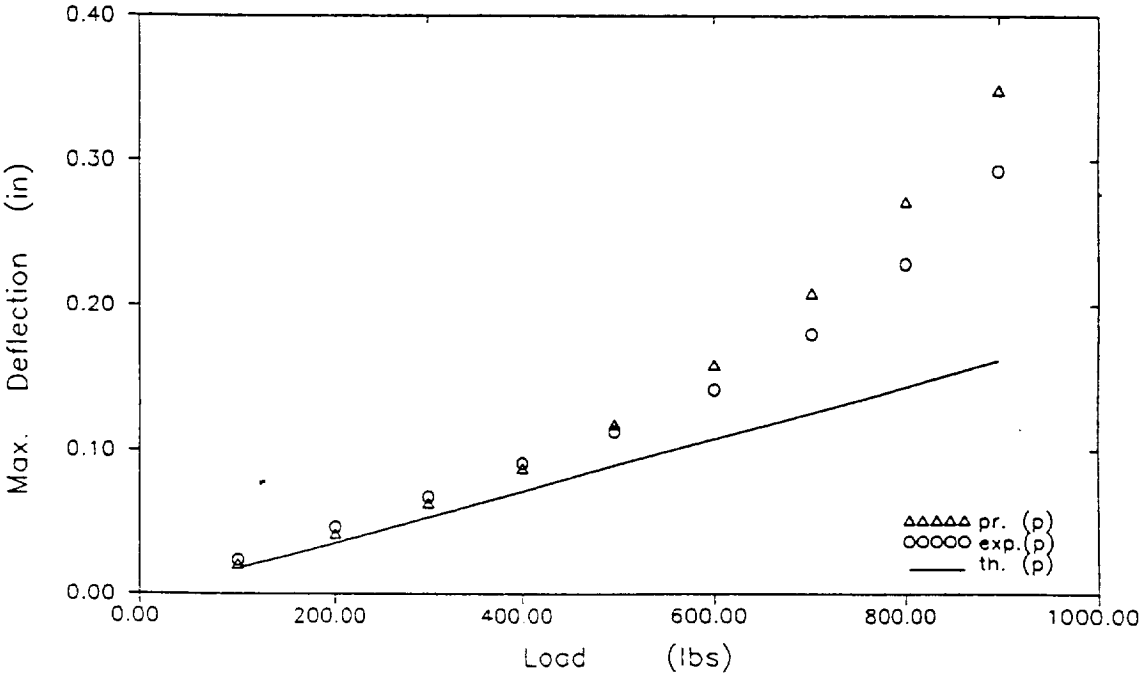

Figure 4.16: *Theoretical, Predicted, and Actual Test Result of Prototype K8* $(0_4/90_4/0_4/90_4/0_4)$ *By Using Model K6* $(0/90/0/...)_{18}$.

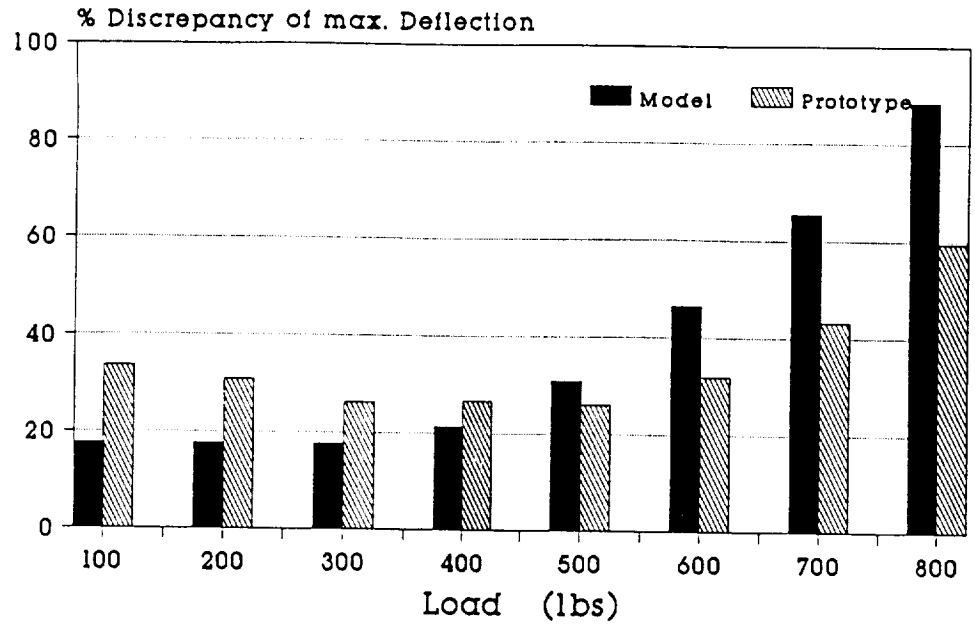

Figure 4.17: *%Discrepancy of Theory and Actual Test Results of Kevlar/Epoxy Plate K8* $(0_4/90_4/0_4/90_4/0_4)$ *and its Model K6* $(0/90/0/...)_{18}$.

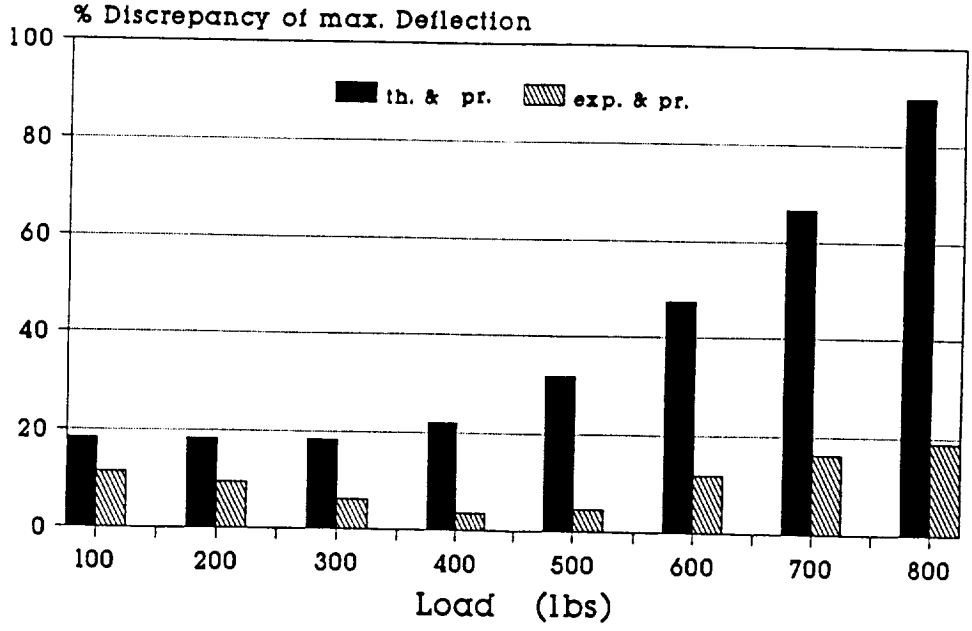

Figure 4.18: *%Discrepancy for Prototype K8* $(0_4/90_4/0_4/90_4/0_4)$ *When Model K6* $(0/90/0/...)_{18}$ is Used.

CASE – 5

In this case, again the Kevlar/Epoxy plate K6 is chosen as the model and the Kevlar/Epoxy plate K9 is its prototype. From the data of Table 4.1 the scale factors are calculated as ;

$$\lambda_a = 1.0 \quad , \quad \lambda_b = 0.9872 \quad , \quad \lambda_h = 0.9184$$

Since the prototype and its model have a different number of plies with different stacking sequences λ_w is

$$\lambda_w = c_d \lambda_a{}^3 \lambda_h{}^{-3} \lambda_q$$

where

$$c_d = \frac{(1404Q_{11} + 54Q_{22})}{(729Q_{11} + 729Q_{22})} \lambda_N{}^{-3}$$

Figures 4.19 and 4.20 show the predicted and actual experimental deflections for different loads. Similar to Case - 4 the predicted data of the prototype match very well with the experimental data, especially for $P \geq 600 lbs$. Beyond this point the theory cannot predict the actual behavior of the prototype (possibly due to fiber or ply failure). Figures 4.21 and 4.22 , which present the % discrepancies for the model and prototype, show this behavior clearly. As the load increases, the discrepancy between theory and experiment for both the model and prototype increase rapidly, while the discrepancy between predicted and experimental values does not change appreciablly. The discrepancies for both model and prototype are shown in Figures 4.21 and 4.22.

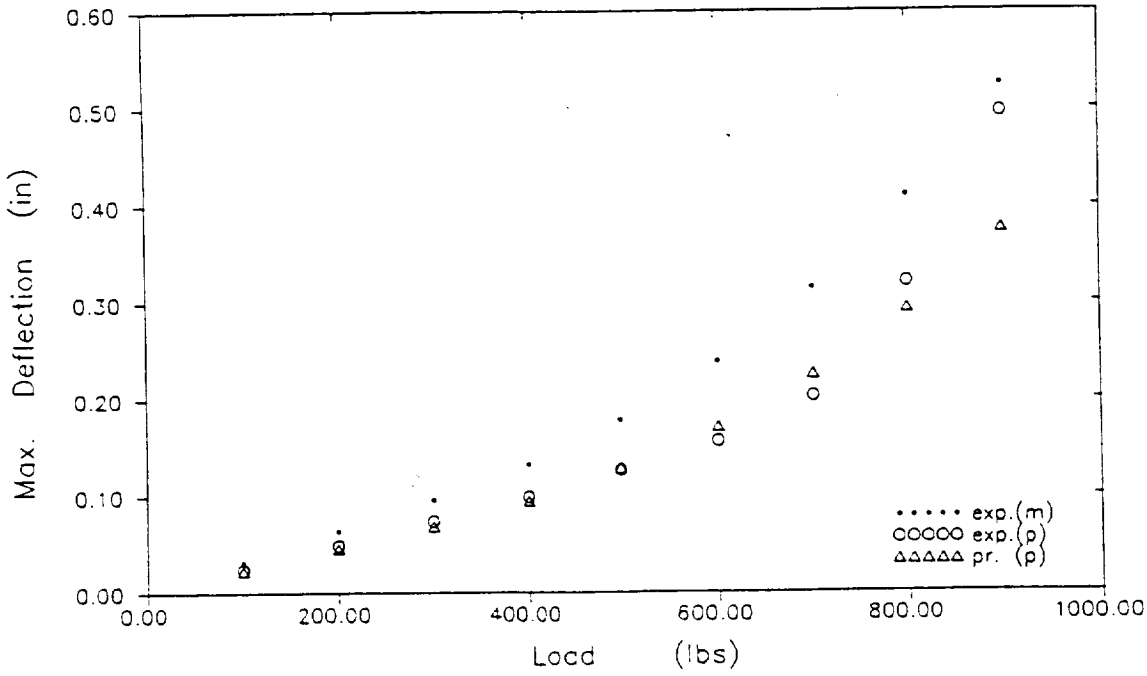

Figure 4.19: *Predicted and Actual Test Results of Kevlar/Epoxy Plate K9* $(0_6/90_6/0_6)$ *and its Model K6* $(0/90/0/...)_{18}$.

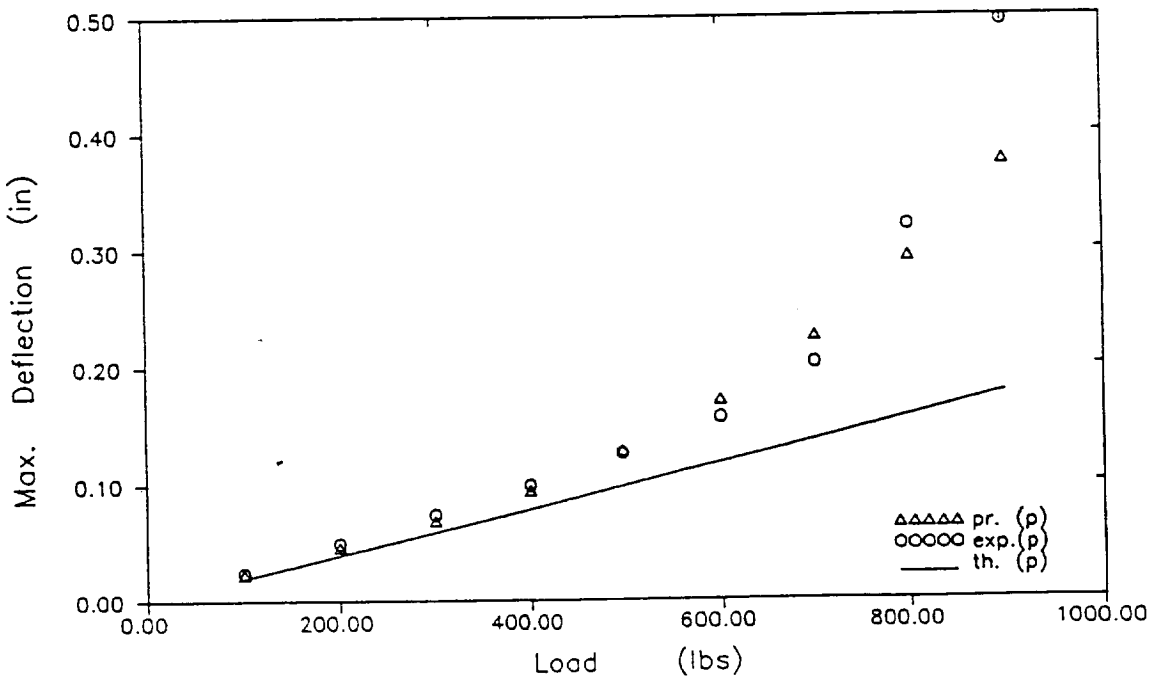

Figure 4.20: *Theoretical, Predicted, and Actual Test Result of Prototype K9* $(0_6/90_6/0_6)$, *By Using Model K6* $(0/90/0/...)_{18}$.

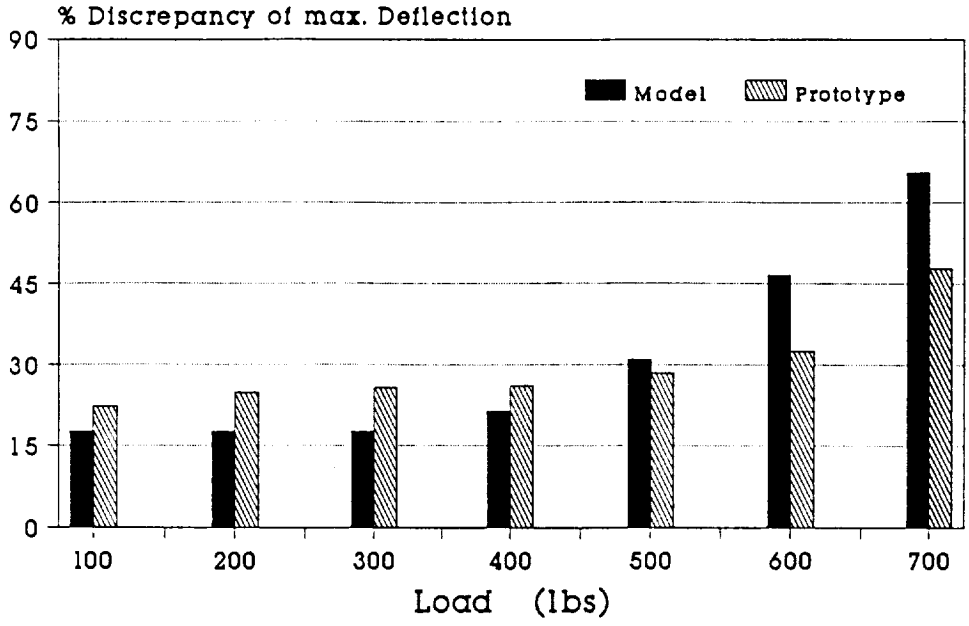

Figure 4.21: *%Discrepancy of Theory and Actual Test Results of Prototype K9* $(0_6/90_6/0_6)$ *and its Model K6* $(0/90/0/...)_{18}$.

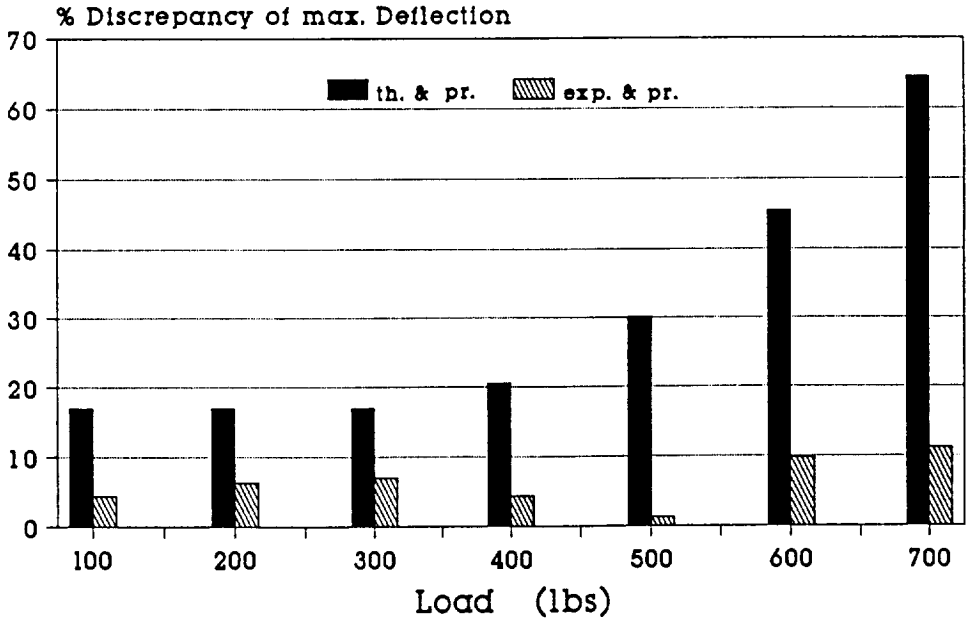

Figure 4.22: *%Discrepancy for Prototype K9* $(0_6/90_6/0_6)$ *When Model K6* $(0/90/0/...)_{18}$ *is Used.*

CASE – 6

In this case the model and prototype have different stacking sequences of the laminae and $\lambda_N \neq 1$. Plate K9 is the prototype and K8 is chosen as its scale model. From the data of Table 4.1 the scale factors are calculated as;

$$\lambda_a = 1.0 \quad , \quad \lambda_b = 0.9877 \quad , \quad \lambda_h = 0.9184$$

Since the number of the plies and the stacking sequence of the laminates are not identical, then λ_w is

$$\lambda_w = c_d \lambda_a{}^3 \lambda_h{}^{-3} \lambda_q$$

where

$$c_d = \frac{(1404Q_{11} + 54Q_{22})}{(1584Q_{11} + 416Q_{22})} \lambda_N{}^{-3}$$

Similar to the other cases Figures 4.23 and 4.24 show the maximum deflections. The predicted values for the prototype match very well with the experimental data, especially for $P < 600lbs$. Beyond this point, the theory cannot predicted the actual behavior of the prototype. Figures 4.25 and 4.26, which represent the % discrepancy for model and prototype, show this behavior clearly. As the load increases, the discrepancy between theory and experiment for both the model and prototype increases , while the discrepancy between the predicted and experimental values increases at a slower rate.

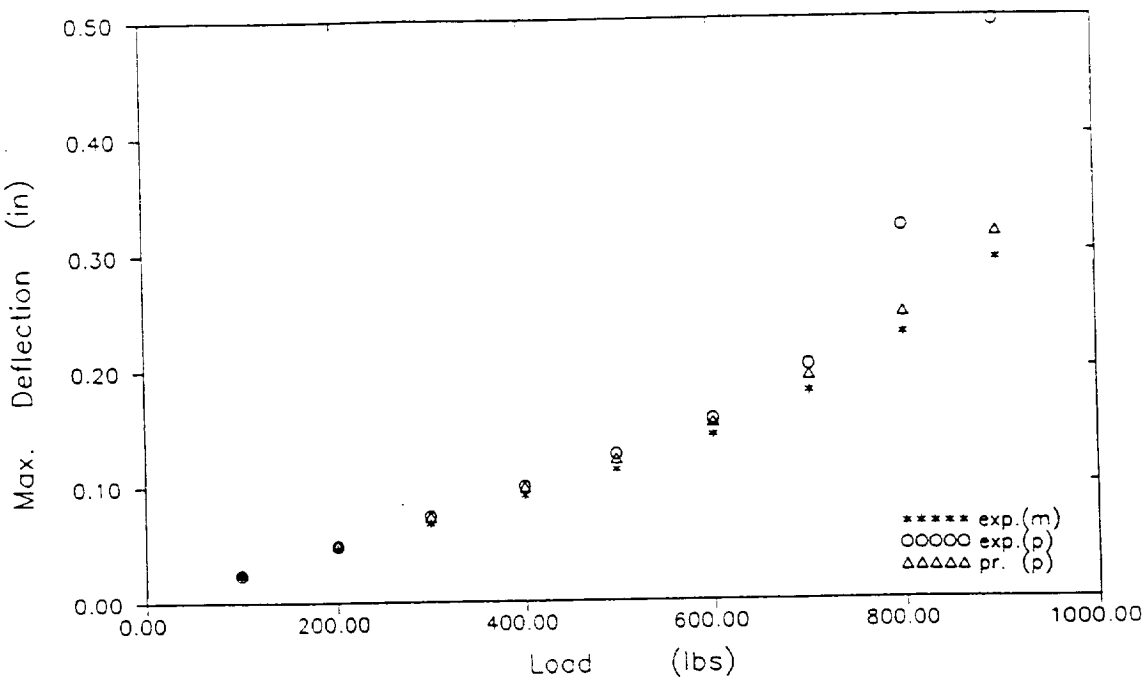

Figure 4.23: *Predicted and Actual Test Results of Kevlar/Epoxy Plate K9* $(0_6/90_6/0_6)$ *and its Model K8* $(0_4/90_4/0_4/90_4/0_4)$

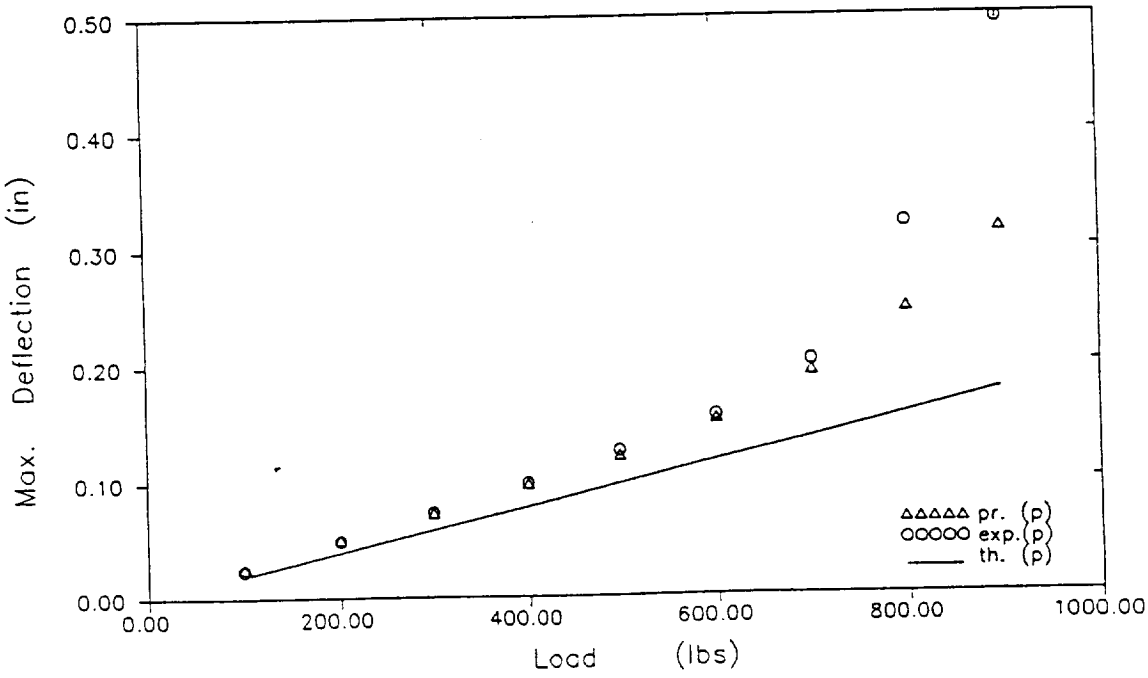

Figure 4.24: *Theoretical, Predicted, and Actual Test Result of Prototype K9* $(0_6/90_6/0_6)$*, By Using Model K8* $(0_4/90_4/0_4/90_4/0_4)$.

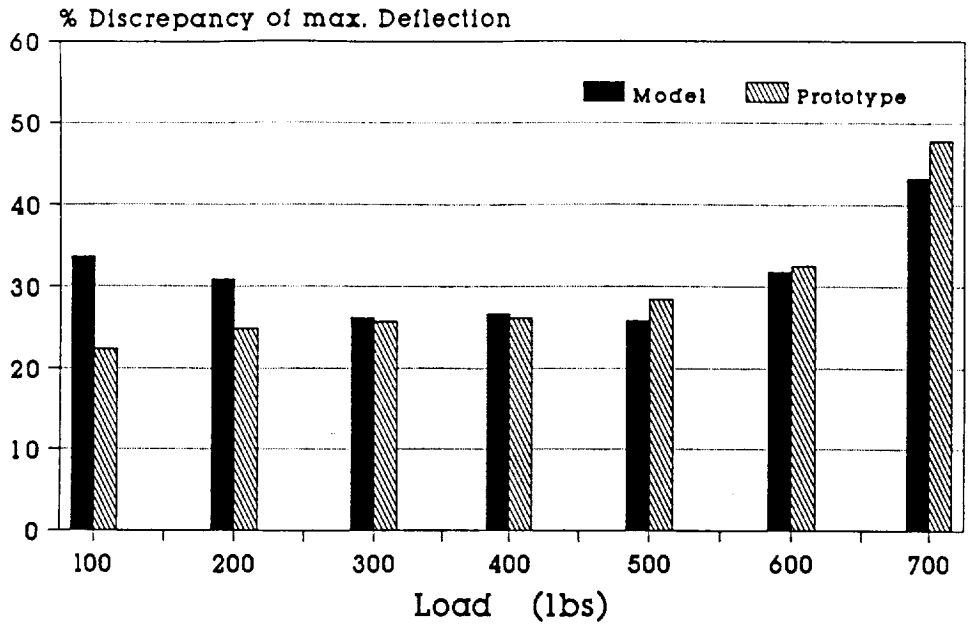

Figure 4.25: *%Discrepancy of Theory and Actual Test Results of Prototype K9* $(0_6/90_6/0_6)$ *and its Model K8* $(0_4/90_4/0_4/90_4/0_4)$.

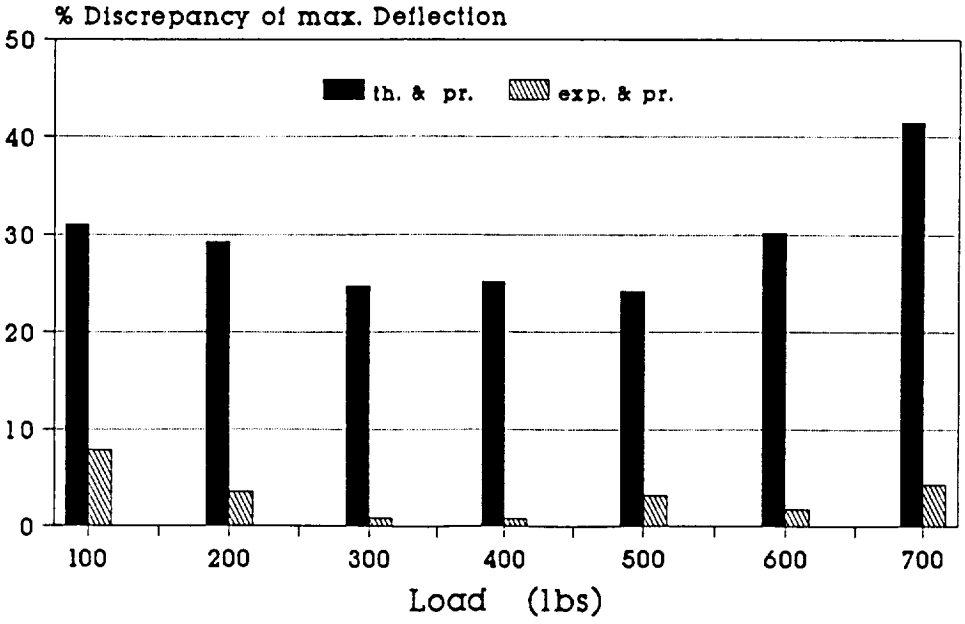

Figure 4.26: *%Discrepancy for Prototype K9* $(0_6/90_6/0_6)$ *When K8* $(0_4/90_4/0_4/90_4/0_4)$ *is Used as Model.*

4.5 Stresses

For the k^{th} lamina, the stresses in terms of the strains and curvatures are;

$$\left\{ \begin{array}{c} \sigma_{xx} \\ \sigma_{yy} \\ \tau_{xy} \end{array} \right\}^{(k)} = \left[\begin{array}{ccc} \bar{Q}_{11} & \bar{Q}_{12} & \bar{Q}_{14} \\ \bar{Q}_{12} & \bar{Q}_{22} & \bar{Q}_{24} \\ \bar{Q}_{14} & \bar{Q}_{24} & \bar{Q}_{44} \end{array} \right]^{(k)} \left(\left\{ \begin{array}{c} {\epsilon^0}_{xx} \\ {\epsilon^0}_{yy} \\ {\gamma^0}_{xy} \end{array} \right\} + z \left\{ \begin{array}{c} k_{xx} \\ k_{yy} \\ k_{xy} \end{array} \right\} \right) \tag{4.29}$$

Where ${\epsilon^0}_{xx}, {\epsilon^0}_{yy}, and {\gamma^0}_{xy}$ are the extensional and shear strains on the reference surface($z = 0$) and k_{xx}, k_{yy}, k_{xy} represent the change in curvature of the reference surface. The $\bar{Q}_{ij}$ are constant for a given lamina. In the case of cylindrical bending ($u = u(x), v = 0, w = w(x)$) ${\epsilon^0}_{yy} = {\gamma^0}_{xy} = k_{yy} = k_{xy} = 0$ which yields

$$\left\{ \begin{array}{c} \sigma_{xx} \\ \sigma_{yy} \\ \tau_{xy} \end{array} \right\}^{(k)} = \left[\begin{array}{ccc} \bar{Q}_{11} & \bar{Q}_{12} & \bar{Q}_{14} \\ \bar{Q}_{12} & \bar{Q}_{22} & \bar{Q}_{24} \\ \bar{Q}_{14} & \bar{Q}_{24} & \bar{Q}_{44} \end{array} \right]^{(k)} \left(\left\{ \begin{array}{c} {\epsilon^0}_{xx} \\ 0 \\ 0 \end{array} \right\} + z \left\{ \begin{array}{c} k_{xx} \\ 0 \\ 0 \end{array} \right\} \right) \tag{4.30}$$

or

$$\left\{ \begin{array}{c} \sigma_{xx} \\ \sigma_{yy} \\ \tau_{xy} \end{array} \right\}^{(k)} = \left\{ \begin{array}{c} \bar{Q}_{11} \\ \bar{Q}_{12} \\ \bar{Q}_{14} \end{array} \right\}^{(k)} \left({\epsilon^0}_{xx} + z k_{xx} \right) \tag{4.31}$$

by substituding the expressions for ${\epsilon^0}_{xx}$ and k_{xx}

$$\left\{ \begin{array}{c} \sigma_{xx} \\ \sigma_{yy} \\ \tau_{xy} \end{array} \right\}^{(k)} = \left\{ \begin{array}{c} \bar{Q}_{11} \\ \bar{Q}_{12} \\ \bar{Q}_{14} \end{array} \right\}^{(k)} \left(u_{,x} + \frac{1}{2} w_{,x}^2 - z w_{,xx} \right) \tag{4.32}$$

$${\sigma_{xx}}^{(k)} = \bar{Q}_{11}^{(k)} \left(u_{,x} + \frac{1}{2} w_{,x}^2 - z w_{,xx} \right) \tag{4.33}$$

Applying similitude theory for the normal stress, σ_{xx},

$$\lambda_{{\sigma_{xx}}^{(k)}} = \lambda_{\bar{Q}_{11}^{(k)}} \left(\frac{\lambda_u}{\lambda_x} + \frac{\lambda_w^2}{\lambda_x^2} - \lambda_z \frac{\lambda_w}{\lambda_x^2} \right) \tag{4.34}$$

The resulting similarity conditions are;

$$\lambda_{{\sigma_{xx}}^{(k)}} = \lambda_{\bar{Q}_{11}^{(k)}} \lambda_u \lambda_x^{-1} \tag{4.35}$$

$$\lambda_{{\sigma_{xx}}^{(k)}} = \lambda_{\bar{Q}_{11}^{(k)}} \lambda_w^2 \lambda_x^{-2} \tag{4.36}$$

$$\lambda_{{\sigma_{xx}}^{(k)}} = \lambda_{\bar{Q}_{11}^{(k)}} \lambda_z \lambda_w \lambda_x^{-2} \tag{4.37}$$

where $\lambda_w = \lambda_x^3 \lambda_q \lambda_{D_{11}}$ and $\lambda_u = \lambda_w \lambda_x \lambda_{B_{11}} \lambda_{A_{11}}^{-1}$

To find which one of Eqs.(4.35)−(4.37) gives the best prediction for the prototype behavior, the theoretical stress of the model is projected with each condition and compared to theoretical stress of the prototype. In this study, the theoretical stress (σ_{xx}) of the model is considered as experimental stress of the model. This stress is projected by using derived similarity conditions, Eqs.(4.35)−(4.37), in order to predict the pertinent stress of the prototype.

For complete similarity, Eqs.(4.35)−(4.37) give the same result. However, for the distorted model each similarity condition gives different results. Figures 4.27– 4.34 present the predicted and theoretical distributions of the normal stress σ_{xx} in various layers of the prototype for cylindrical bending test. It is observed that the predicted stresses by Eq.(4.37) agree very well with the theoretical results. Eq.(4.36) cannot predict the behavior of the prototype accurately. Eq.(4.35) is not a suitable similarity condition, since its predicted data do not match the theoretical results. The figures do not include the predicted stresses using Eq.(4.35). The predicted stresses using Eq.(4.36) are not included in all the figures. This is purposely done in order to simplify the figures.

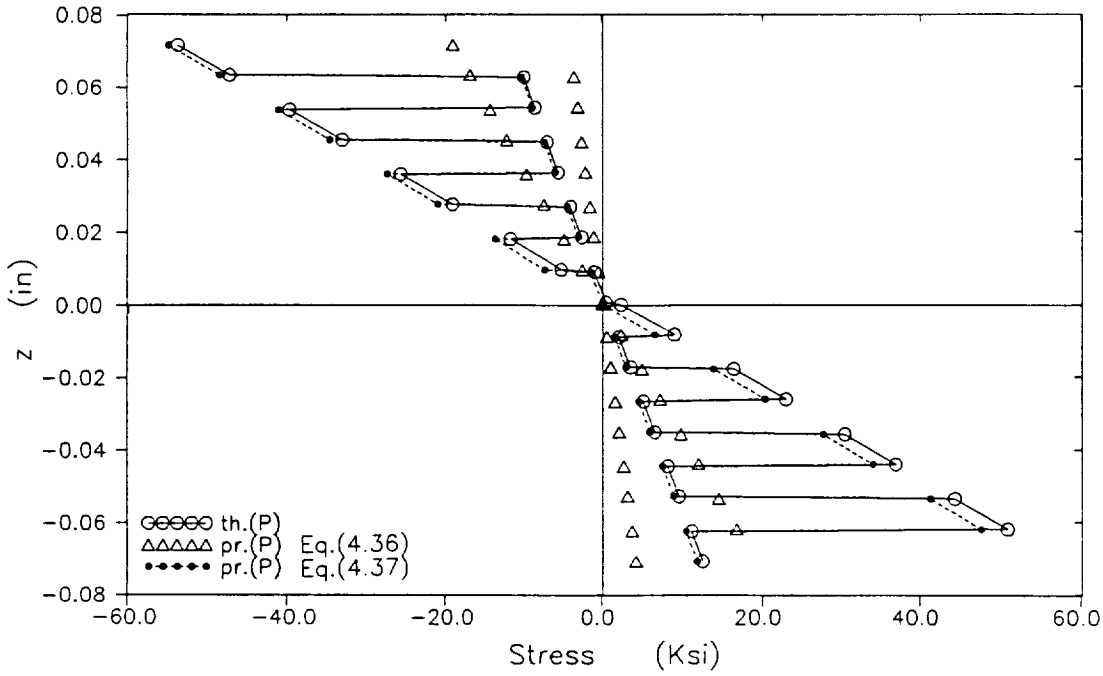

Figure 4.27: *Predicted and Theoretical Normal Stress σ_{xx} Distributions in Various Layers of the Prototype G1* $(0/90/0...)_{16}$ *When G3* $(0_3/90_3/0_3/90_3/0_3)$ *Is Used as Model.*

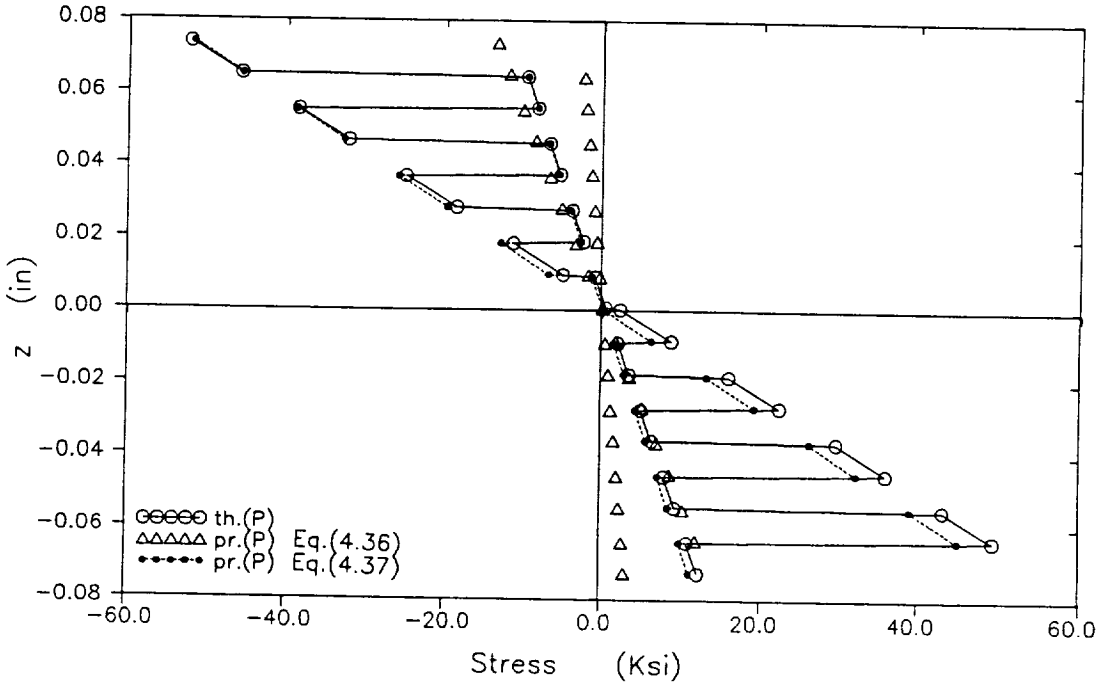

Figure 4.28: *Predicted and Theoretical Normal Stress σ_{xx} Distributions in Various Layers of the Prototype G2* $(0/90/0...)_{16}$ *When G4* $(0_3/90_3/0_3/90_3/0_3)$ *Is Used as Model.*

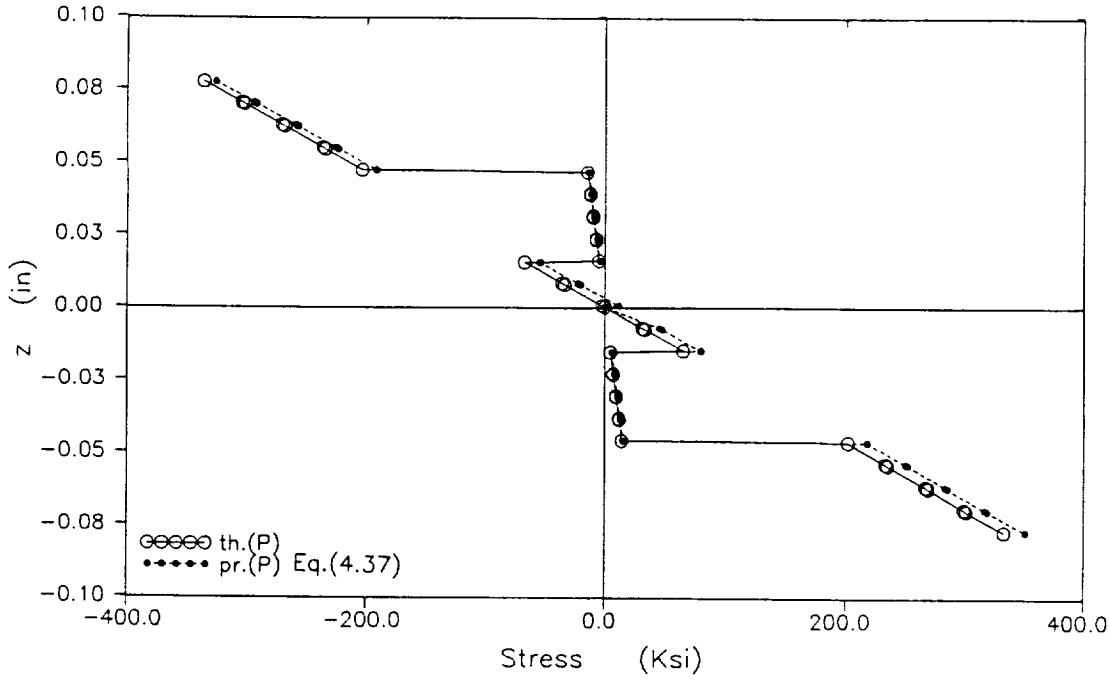

Figure 4.29: *Predicted and Theoretical Normal Stress σ_{xx} Distributions in Various Layers of the Prototype K7* $(0_4/90_4/0_4/90_4/0_4)$ *When G1* $(0/90/0...)_{16}$ *Is Used as Model.*

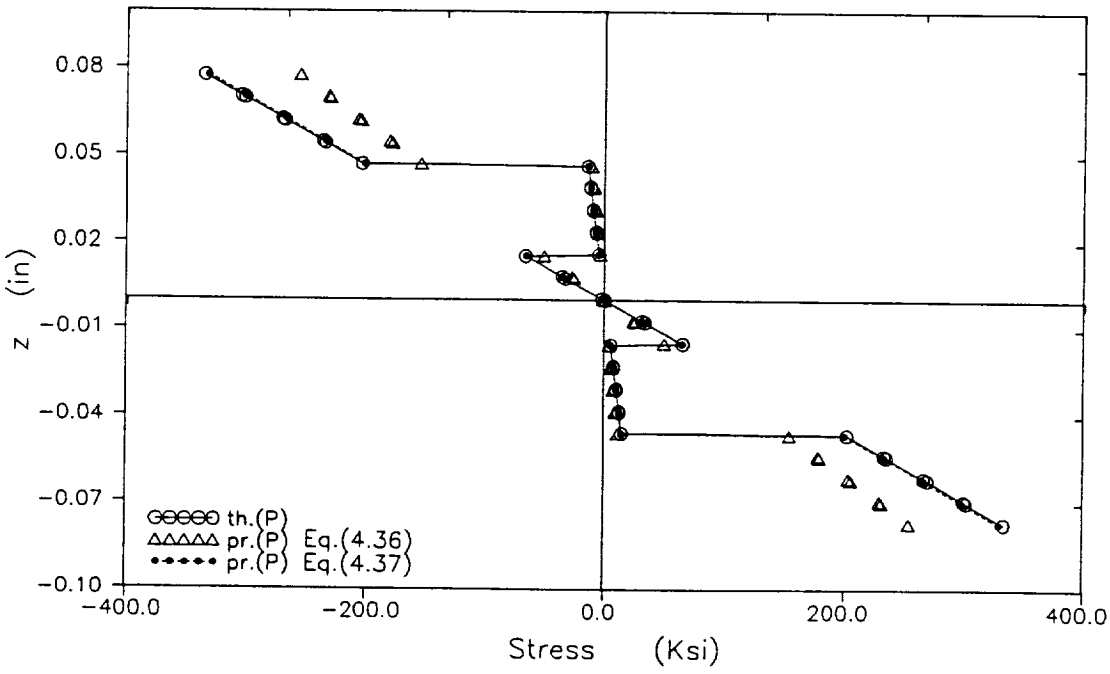

Figure 4.30: *Predicted and Theoretical Normal Stress σ_{xx} Distributions in Various Layers of the Prototype K7* $(0_4/90_4/0_4/90_4/0_4)$ *When G4* $(0_3/90_3/0_3/90_3/0_3)$ *Is Used as Model.*

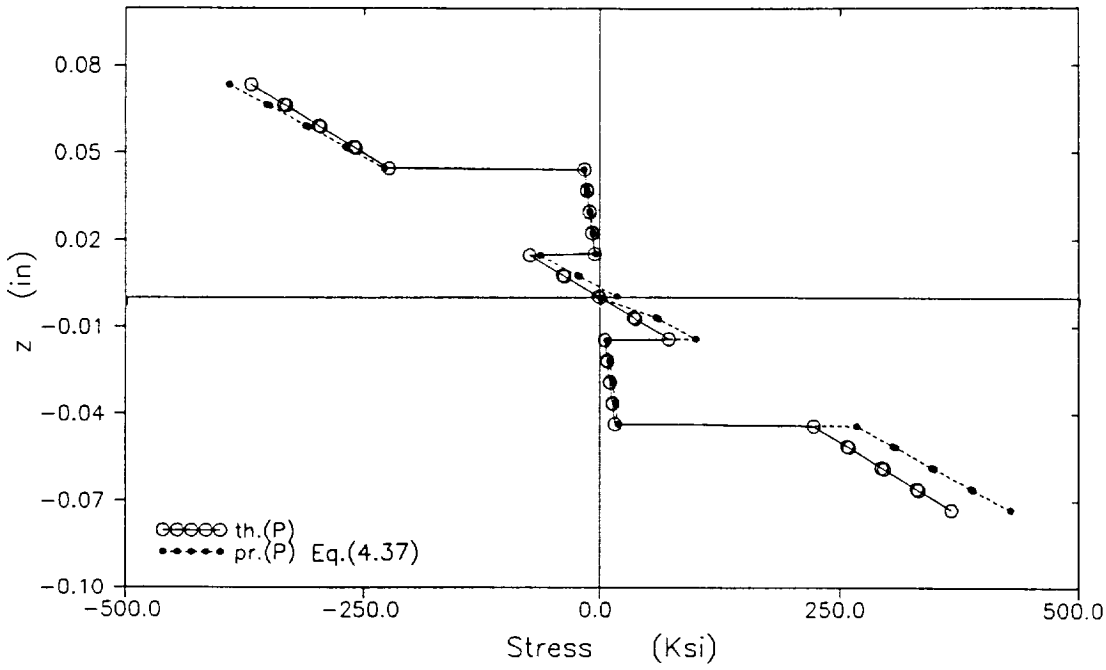

Figure 4.31: *Predicted and Theoretical Normal Stress σ_{xx} Distributions in Various Layers of the Prototype K8* $(0_4/90_4/0_4/90_4/0_4)$ *When K6* $(0/90/0...)_{18}$ *Is Used as Model.*

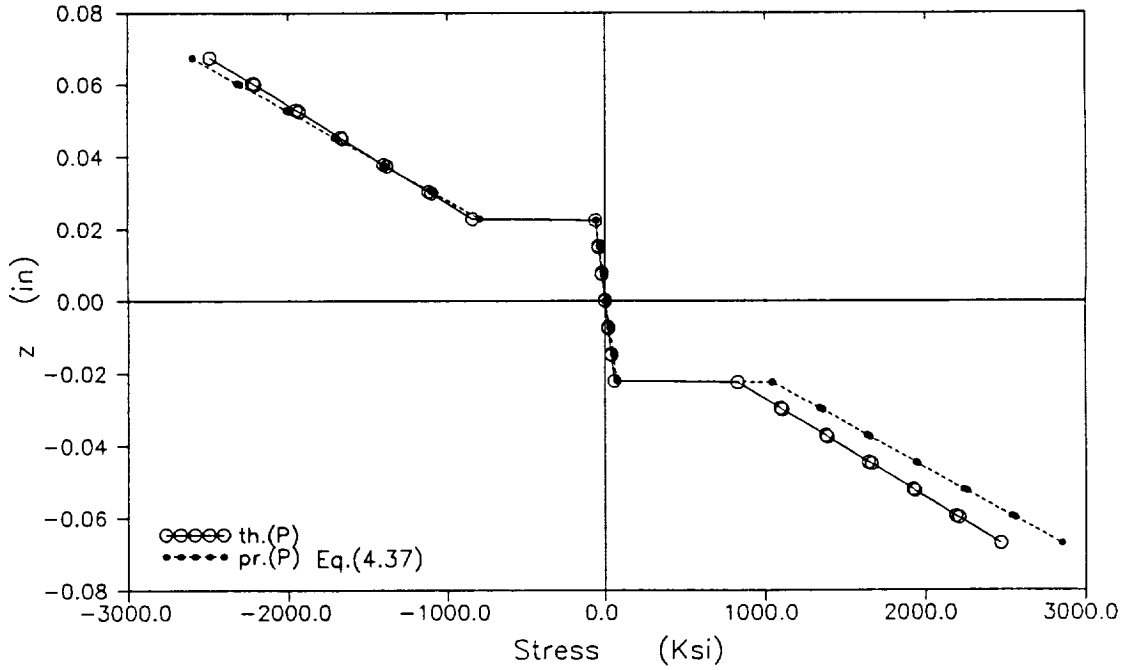

Figure 4.32: *Predicted and Theoretical Normal Stress σ_{xx} Distributions in Various Layers of the Prototype K9* $(0_6/90_6/0_6)$ *When K6* $(0/90/0...)_{18}$ *Is Used as Model.*

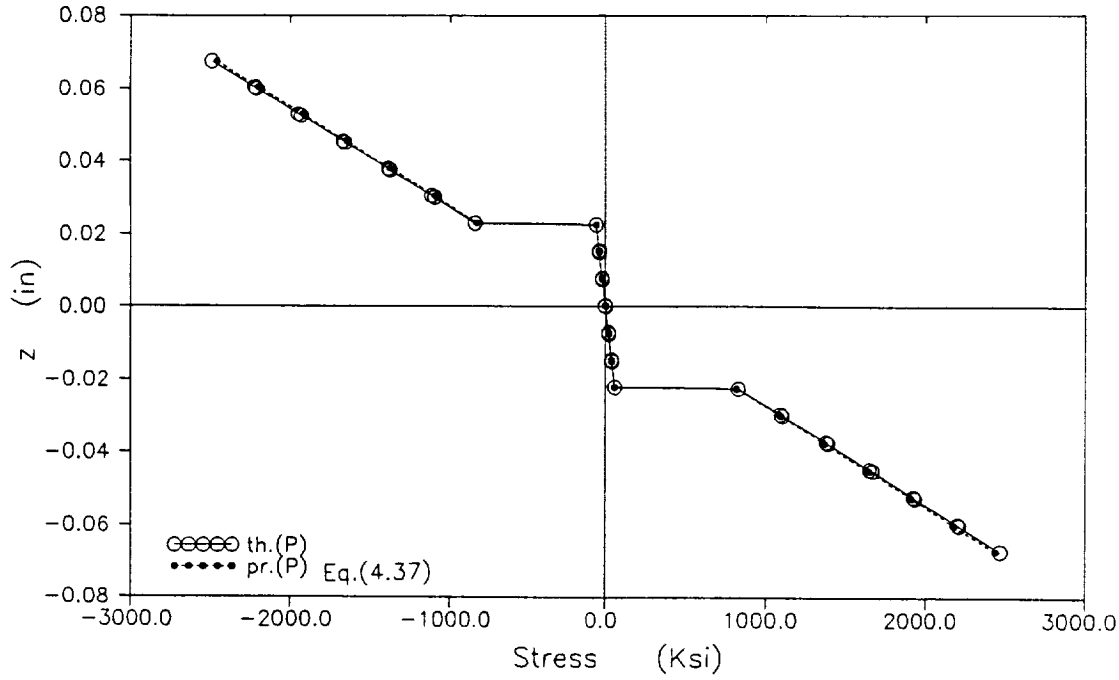

Figure 4.33: *Predicted and Theoretical Normal Stress σ_{xx} Distributions in Various Layers of the Prototype K9* $(0_6/90_6/0_6)$ *When K8* $(0_4/90_4/0_4/90_4/0_4)$ *Is Used as Model.*

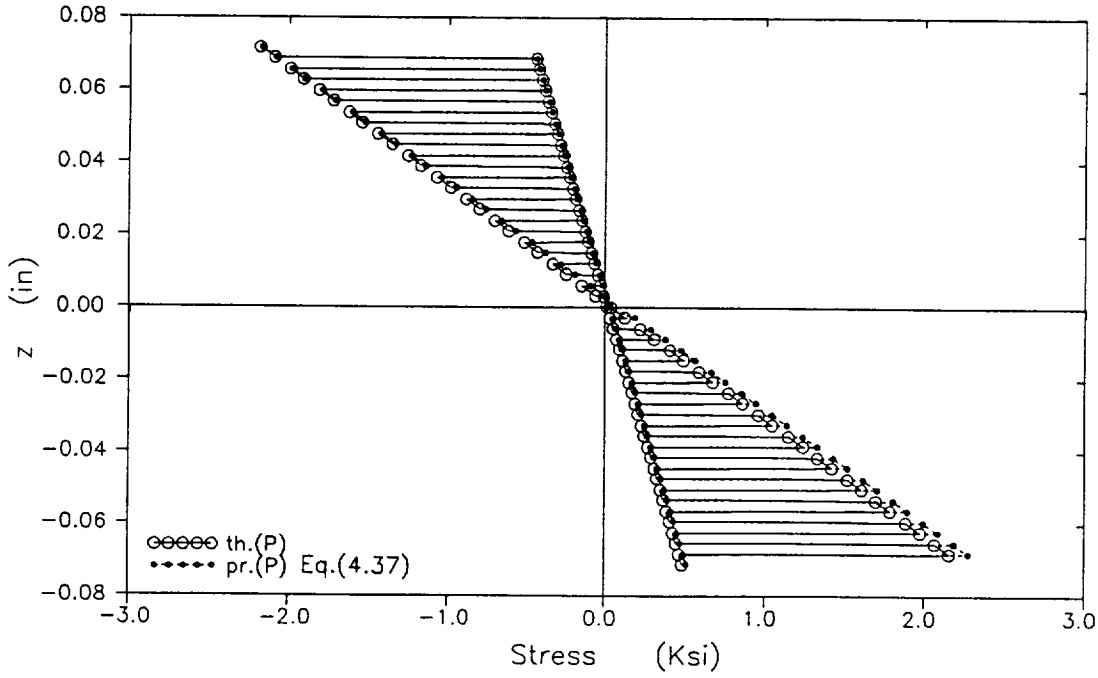

Figure 4.34: *Predicted and Theoretical Normal Stress σ_{xx} Distributions in Various Layers of the Prototype G5* $(0/90/0...)_{48}$ *When G1* $(0/90/0...)_{16}$ *Is Used as Model.*

REFERENCES

1. Ashton, J.E. and Whitney J. M. (1970), *Theory Of Laminated Plates* , Technomic Publ. Co. Stamford, Conn.

2. Barr, D.I.H. (1979), " Echelon matrix in dimensional analysis ", *Int'l J. of Mechanical Eng. Education* , Vol.7, pp 85 - 89.

3. Barr, D.I.H.(1983), "A survey of procedures for dimensional analysis", *Int'l J. of Mechanical Eng. Education* , Vol. 11, pp 147 - 159.

4. Charturverdi, S and Sierakowski, R.L. (1991), Private communications, Department of Civil Engineering , The Ohio State Univ. , Columbus , Ohio.

5. Goodier, J.N. and Thomson, W.T. (1944) ," Applicability of similarity principles to structural model", NACA Tech. Note 933.

6. Goodier, J.N. (1950)," Dimensional analysis " ,*Handbook of experimental stress analysis* , edited by M. Hetenyi , Wiley & Sons Inc. New York pp 1035 - 1045.

7. Harris, H. S., Sabnis, G. M. and White, R. N.(1970), "Reinforcement for small scale direct models of concrete structures", Paper NO. SP-24-6, *Model for Concrete Structures*, ACI SP-24, American Concrete Institude, Detroit, Mich., PP. 141-148.

8. Harris, H. S., Sabnis, G. M. and White, R. N.(1967), " Small scale ultimate strength models of concrete structures, paper presented at SESA annual meeting.

9. Hsu, S. T., Griffin, J. H. and Bielak, J. (1989), " How gravity and joint scaling affect dynamic response ", *AIAA J.*, Vol. 27, No. 9, PP 1280 - 1287.

10. Krawinkler, H., Mills, R. S. and Moncarz, P. D. (1978), " Scale modeling and testing of structures for reproducting response to earthquake excitation", Tech-